

ORIGINAL RESEARCH

Candidate genes for limiting cholestatic intestinal injury identified by gene expression profiling

Samuel M. Alaish¹, Jennifer Timmons¹, Alexis Smith¹, Marguerite S. Buzza², Ebony Murphy¹, Aiping Zhao³, Yezhou Sun⁴, Douglas J. Turner⁵, Terez Shea-Donahue^{2,3}, Toni M. Antal^{1,2}, Alan Cross³ & Susan G. Dorsey⁶

¹ Department of Surgery, University of Maryland School of Medicine, Baltimore, Maryland

² Department of Physiology, University of Maryland School of Medicine, Baltimore, Maryland

³ Department of Medicine, University of Maryland School of Medicine, Baltimore, Maryland

⁴ Institute for Genome Sciences, University of Maryland School of Medicine, Baltimore, Maryland

⁵ Baltimore Veterans Administration Medical Center, Baltimore, Maryland

⁶ University of Maryland School of Nursing, Baltimore, Maryland

Keywords

Cholestasis, growth hormone, intestine, lipocalin, microarray.

Correspondence

Samuel M. Alaish, Department of Surgery, University of Maryland School of Medicine, Room N4E35, 22 South Greene Street, Baltimore, MD 21201.

Tel: (410) 328-5730

Fax: (410) 328-0652

E-mail: salaish@smail.umaryland.edu

Funding Information

Research reported in this publication was supported by the National Institutes of General Medical Sciences of the National Institutes of Health under award number K08GM081701. The content is solely the responsibility of the authors and does not necessarily represent the official views of the National Institutes of Health.

Received: 17 June 2013; Revised: 22 July 2013; Accepted: 1 August 2013

doi: 10.1002/phy2.73

Physiol Rep, 1 (4), 2013, e00073, doi: 10.1002/phy2.73

Abstract

The lack of bile flow from the liver into the intestine can have devastating complications including hepatic failure, sepsis, and even death. This pathologic condition known as cholestasis can result from etiologies as diverse as total parenteral nutrition (TPN), hepatitis, and pancreatic cancer. The intestinal injury associated with cholestasis has been shown to result in decreased intestinal resistance, increased bacterial translocation, and increased endotoxemia. Anecdotal clinical evidence suggests a genetic predisposition to exaggerated injury. Recent animal research on two different strains of inbred mice demonstrating different rates of bacterial translocation with different mortality rates supports this premise. In this study, a microarray analysis of intestinal tissue following common bile duct ligation (CBDL) performed under general anesthesia on these same two strains of inbred mice was done with the goal of identifying the potential molecular mechanistic pathways responsible. Over 500 genes were increased more than 2.0-fold following CBDL. The most promising candidate genes included major urinary proteins (MUPs), serine protease-1-inhibitor (Serpina1a), and lipocalin-2 (LCN-2). Quantitative polymerase chain reaction (qPCR) validated the microarray results for these candidate genes. In an in vitro experiment using differentiated intestinal epithelial cells, inhibition of MUP-1 by siRNA resulted in increased intestinal epithelial cell permeability. Diverse novel mechanisms involving the growth hormone pathway, the acute phase response, and the innate immune response are thus potential avenues for limiting cholestatic intestinal injury. Changes in gene expression were at times found to be not only due to the CBDL but also due to the murine strain. Should further studies in cholestatic patients demonstrate interindividual variability similar to what we have shown in mice, then a “personalized medicine” approach to cholestatic patients may become possible.

Introduction

Cholestasis, defined as little or no bile flow from the liver into the intestine, is a complex pathologic condition that can develop from either functional etiologies, such as hepatic parenchymal disease secondary to hepatitis, or mechani-

cal etiologies, such as an obstructing pancreatic cancer or biliary stricture. In the pediatric population, cholestasis resulting from prolonged parenteral nutrition is by far the most common etiology. Cholestatic injury has not only a hepatic component but also an intestinal one. Failure of the intestinal barrier with decreased intestinal resistance,

increased bacterial translocation, and increased episodes of sepsis has been well described (Campillo et al. 1999; Pascual et al. 2003; Frances et al. 2004); however, the exact mechanisms remain poorly understood.

Common bile duct ligation (CBDL) is a standard model of cholestasis in the literature (Georgiev et al. 2008). CBDL in mice leads to both hepatic and intestinal injuries which are precisely interrelated. We have previously found differences in the systemic inflammatory responses and outcome following CBDL between two inbred mouse strains, C57BL/6J (B6) and A/J, suggesting a genetic contribution (Alaish et al. 2005). In particular, B6 mice were significantly more likely to develop ascites following 1 week of CBDL (Alaish et al. 2005). In concordance with this observation, the frequency of mortality after CBDL was significantly higher in B6 mice compared to A/J mice on days following CBDL (Alaish et al. 2005). Interestingly, although both strains demonstrated markedly elevated plasma liver function tests following CBDL, no difference was noted in liver histology between the two ligated strains. More recently, our laboratory has shown decreased intestinal resistance and increased bacterial translocation following CBDL in these same two strains of inbred mice. Furthermore, we found genetic variation in the intestinal resistance and bacterial translocation rates, which correlated with mortality following CBDL in different strains of inbred mice (Alaish et al. 2013). Further analysis implicated an IFN- γ -mediated apoptotic-independent mechanism of tight junction disruption, which has been well described in vitro (Madara and Stafford 1989; Marano et al. 1998; Youakim and Ahdiieh 1999; Bruewer et al. 2003; Clayburgh et al. 2004), as a mechanism possibly responsible for the genetic variation. Nevertheless, the 2.5-fold changes in IFN- γ gene expression following CBDL, albeit significant, did not seem monumental enough to fully explain the striking genetic influence on mortality following CBDL in the mice. In order to uncover other potential mechanisms including novel pathways, we embarked on a whole-genome microarray analysis of jejunal tissue in these two different strains of inbred mice following either a sham operation or CBDL. The differentially expressed genes reported here constitute a resource of candidate genes for roles in cholestatic intestinal injury.

Material and Methods

Animals

Male A/J and C57BL/6J (B6) mice (8 weeks old) were obtained from the Jackson Laboratory (Bar Harbor, ME) and maintained in identical environmental conditions in a pathogen-free animal facility with 12-h light-dark

cycles. All mice weighed 18–25 g at the time of operation. Matriptase (*St14*) hypomorphic C57BL/6J mice (List et al. 2007) were bred in the Antalis laboratory. Animal studies were conducted according to protocols reviewed and approved by the University of Maryland School of Medicine Institutional Animal Care and Use Committee and adhered to guidelines promulgated by the National Institutes of Health. In accordance with these guidelines, we used the minimum number of animals to meet the rigor necessary for this series of experiments.

Experimental design

CBDL operative procedure

Mice were anesthetized by inhaled isoflurane anesthesia. The abdomen was clipped and then prepared in sterile fashion with 70% ethyl-ethanol followed by betadine. A transverse upper abdominal incision was performed. The CBD was dissected away from the portal vein and was ligated near its junction with the duodenum using aneurysm clips engineered with a precisely standardized opening/closing mechanism. The abdominal wall was then closed in a two-layer fashion using absorbable sutures. Sham-operated mice were treated identically but without dissection or ligation of the CBD. Postoperatively, animals were resuscitated with warmed subcutaneous injections of saline (1 mL) to replace losses. Mice were returned to clean cages where food and water were provided ad libitum. Buprenorphine, 0.05–0.1 mg/kg was given subcutaneously at the time of surgery and then every 8–12 h to treat postoperative pain for 48–72 h.

RNA extraction

Seven days following the surgery, the mice underwent deep general anesthesia and euthanasia by thoracotomy and cardiac exsanguination. Postoperative day 7 was chosen because this time point corresponded to our earlier finding of decreased intestinal transepithelial electrical resistance (TEER) after CBDL (Alaish et al. 2013). In addition, this time point exhibited differences in TEER based on the genetic background of the mouse (Alaish et al. 2013). These TEER findings were found in both the jejunum and ileum and correlated with differences in bacterial translocation and mortality. Further studies on jejunal tissue demonstrated differences in tight junction protein expression between CBDL and sham animals and between the strains (Alaish et al. 2013). Therefore, in this study, we chose jejunum once again; the intestinal tissue was harvested under sterile conditions. RNA extraction and purification were performed as we have previously described (Dorsey et al. 2009).

Microarray data analysis

Microarray expression profiling was performed according to the manufacturer protocols (Affymetrix, Santa Clara, CA). Briefly, total RNA was used to prepare biotinylated cRNA, followed by fragmentation and hybridization to Affymetrix arrays (Genechip Mouse 430 2.0; Affymetrix, Santa Clara, CA). The arrays were incubated for approximately 16 h, washed, stained, and scanned per Affymetrix. Differential gene expression through microarray was then performed. We utilized .cel files generated from Affymetrix profiling process for analysis. Arrays were normalized by GCRMA method implemented in gcrma R package (Bioconductor, an open source collection of software packages). Differential expression analysis was performed using limma R package (Bioconductor). First, a linear model was fitted to expression data for each gene. Empirical Bayes method was then used to assess differential expression between two conditions. A cutoff of FDR less than 0.05 was used to select significant probes. A complete data set has been submitted to the NCBI Gene Expression Omnibus (NCBI GEO #GSE47099 and NCBI Tracking System #16793295).

qPCR verification of promising candidate genes

The identification of significant changes in expression of promising candidate genes (major urinary proteins [MUPs], serine protease-1-inhibitor [Serpina1a] and lipocalin-2 [LCN2]) through microarray analysis was validated using a quantitative polymerase chain reaction (qPCR) technique. Total RNA was isolated from homogenized jejunal samples that were stored in TRIzol (Invitrogen, Grand Island, NY). The total RNA was isolated from TRIzol samples as per the manufacturer's instructions. The pellet was allowed to air dry, and the total RNA was resuspended in an appropriate volume of RNase-free water. RNA concentrations were calculated using a NanoDrop 1000 spectrophotometer (Thermo Scientific, Waltham, MA). Single-stranded cDNA was synthesized from 2 μ g of total RNA using random hexamer primer and the First-Strand cDNA Synthesis Kit (MBI Fermentas, Hanover, MD). The specific primer sequences were designed using Beacon Designer 7.0 (Premier Biosoft International, Palo Alto, CA) and synthesized by the University of Maryland School of Medicine Biopolymer/Genomics Core. qPCR reactions were set up using iQ SYBR Green Supermix (Bio-Rad, Hercules, CA) in a total volume of 25 μ L. Amplification conditions were as follows: 95°C for 3 min, 50 cycles of 95°C for 15 sec, 60°C for 15 sec, and 72°C for 20 sec. All reactions were performed using Bio-Rad iCycler instrumentation and software. All samples were normalized with 18s rRNA housekeeping gene

levels with subsequent calculation of fold change in mRNA expression. Analysis was carried out in GraphPad Prism5 (San Diego, CA, USA).

Mortality following CBDL in matriptase hypomorphic B6 mice

We conducted a mortality study following CBDL in wild-type C57BL/6J mice ($n = 8$) and matriptase (*St14*) hypomorphic C57BL/6J mice ($n = 11$). Sham-operated mice of each strain served as controls.

Cells

Cdx2-intestinal epithelial cells (Cdx2-IEC), a transformed rat crypt IEC-6 cell line which maintains a stable differentiated phenotype upon future passages, were obtained from Dr. J.-Y. Wang (University of Maryland, Baltimore, MD). Cdx2-IEC cells were maintained at 37°C in a humidified incubator with 10% CO₂ in DMEM containing 5% (v:v) fetal bovine serum (FBS), 0.5% (v:v) ITS + liquid media supplement, 0.1 million units/L penicillin, 100 mg/L streptomycin, and 4 mmol/L soprolythio- β -D-galactoside, which served as an inducer.

Transfection of Cdx2-IEC cells with MUP-1 siRNA and FITC-dextran permeability assay

Following their sixth passage, Cdx2-IEC cells were transfected with either MUP-1 siRNA (Thermo Scientific, Inc.) or Acell Control Non-Targeting siRNA (Thermo Scientific, Inc.) as described previously (Rao et al. 2006). The siRNAs used were as follows: 80 nmol/L Control siRNA; and 20 nmol/L, 40 nmol/L, and 60 nmol/L MUP-1 siRNA. Silencing of MUP-1 in the cells was confirmed by Western blot analysis using MUP (F-3) mouse monoclonal antibody (Santa Cruz Biotechnology, Inc., Paso Robles, CA, USA). Six-well transwell plates with 12-mm-diameter inserts (Costar 3407; Corning, Inc., Kennebunk, ME, USA) were used to perform the permeability studies following the transfection. The cells were incubated on the inserts with control media for 24 h to allow proper attachment to the membrane prior to dextran administration. After 24 h, TEER was measured in both control and transfected Cdx2-IEC cells for the formation of the monolayer as described previously (El Asmar et al. 2002). The media were removed. 4-kDa FITC-dextran in control media was placed onto the apical side (top chamber); control media alone was placed on the basolateral side. The TEER was monitored for 2 h and 100- μ L aliquots of the basolateral medium were collected after each 30-min time period. A sample from the top compartment at the time of the last sampling of the bottom compartment was

used to normalize the samples to account for possible differences in the total fluorescence added at the beginning of the experiment. Fluorescence of the samples was quantified in a multiplate fluorescence reader in black 96-well plates; the excitation wavelength was 485 nm and emission wavelength was 538 nm.

Statistical analysis

The microarray data (reported as percent change) were analyzed using repeated measures analyses of variance (ANOVA) with false discovery rate correction to control multiple testing errors. Post hoc testing was done using Tukey's honestly significant difference (HSD). qPCR data were analyzed using ANOVA with the Bonferroni post-test. Graph Pad Prism 5 software was used. For the matriptase hypomorphic B6 mouse CBDL experiment, a Kaplan–Meier survival curve was generated with $P < 0.05$ considered as significant.

Results

Microarray data

As shown in Figure 1A, more than 500 genes were significantly differentially regulated in the CBDL mice compared with sham. When examining changes across strains, although there are shared genes, there are a significant number of differentially regulated genes that are unique to each strain (Fig. 1B). Table 1 shows the number of genes in each category. The first two lines of data in Table 1 demonstrate that many more genes are differentially expressed in A/J mice as compared to B6 mice following CBDL (582 vs. 137). The last two lines of data in Table 1 demonstrate that there are more genes undergoing expression changes following CBDL compared to sham (882 vs. 766). In Figure 1C, the heat map shows clustering of all differentially expressed genes by genotype. A list of all differentially expressed genes can be found in Table A1. In Figure 1D, the top 53 significantly regulated genes across the two strains are shown in a separate heat map (For both heat maps, red = upregulated genes; green = downregulated genes). Note the disparate gene expressions in the two strains.

We next examined significantly enriched canonical signaling pathways. First, we evaluated those that were unique within a strain in the CBDL condition compared with sham. As shown in Figure 2A, coagulation pathways were highly upregulated in A/J CBDL mice compared with sham. In contrast, coagulation pathways were not significantly regulated in B6 CBDL versus sham (Fig. 2B). In Figure 2C, we show that there are a number of signaling pathways that are differentially regulated in A/J CBDL

compared with B6 CBDL, demonstrating differential pathway activation in CBDL across these two inbred strains of mice.

qPCR verifies microarray results of candidate genes

The following genes struck us as particularly promising as candidate genes to limit cholestatic injury: MUPs, Serpina1a, and LCN2. They all had significant changes in gene expression following CBDL. MUPs and Serpina1a also had disparate strain expressions which could account for the phenotypic differences we see following ligation. LCN2 was chosen because it is known to play a protective role in the intestinal barrier (Berger et al. 2006). Although we did not see strain differences in LCN2, we did find striking differences between the sham and CBDL mice, which we believe is an important finding. This study not only illustrates strain differences following CBDL but also serves to illustrate intestinal gene expression changes following CBDL independent of strain. qPCR did, indeed, verify our results for MUPs, Serpina1a, and LCN2. (Fig. 3A–C).

Matriptase (St14) hypomorphic B6 mice do not have significantly increased mortality following CBDL compared to wild-type B6 mice

Serpina1a is a serine protease inhibitor, suggesting that decreased intestinal serine protease activity could contribute to the decreased intestinal resistance associated with CBDL. Matriptase is a serine protease whose loss results in decreased intestinal resistance as measured by decreased intestinal TEER (Buzza et al. 2010). We hypothesized that when coupled with the loss of matriptase, the increase in Serpina1a which follows CBDL would result in such a large drop in intestinal resistance that mortality would increase. Although there appeared to be a trend toward increased mortality in the matriptase (*St14*) hypomorphic B6 mice early on following CBDL, this difference never became significant and did not persist, as can be seen in the Kaplan–Meier Survival Curve (Fig. 4).

MUP-1 siRNA transfection increases permeability in Cdx2-IEC cells

Growth hormone treatment has beneficial effects on the intestine by normalizing intestinal permeability (Liu et al. 2003). We hypothesize that increased expression of MUPs by growth hormone activation (Kuhn et al. 1984) could contribute to this beneficial effect. We inhibited MUP-1 protein expression using siRNA technology. Following confirmation of inhibition of MUP-1 protein expression

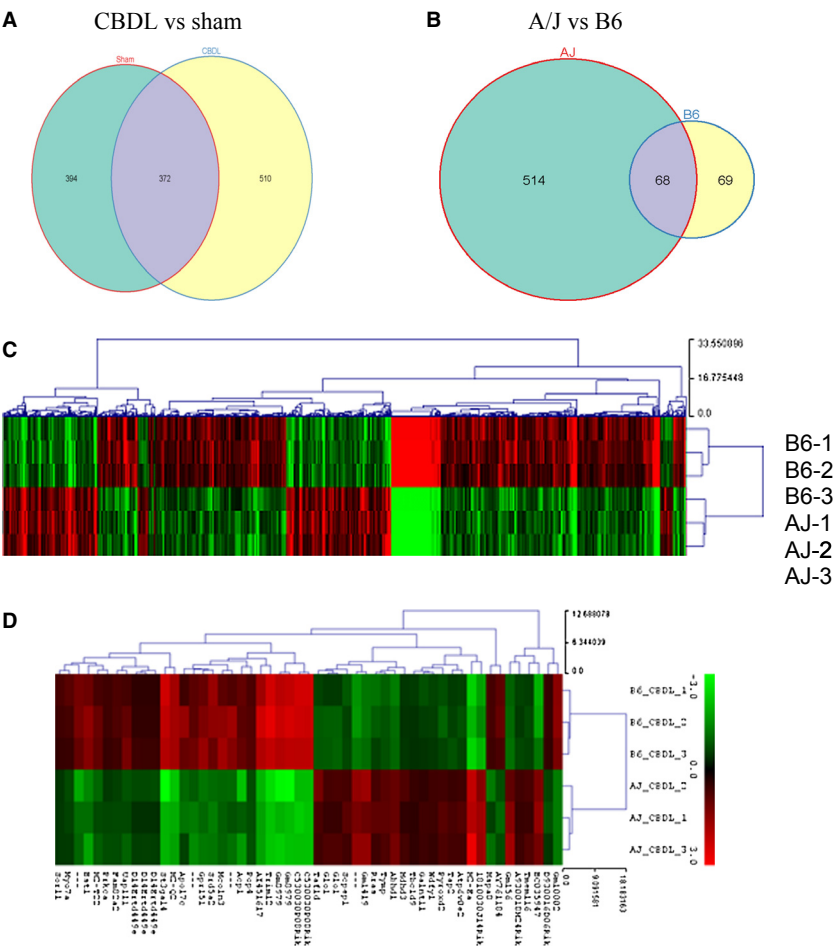


Figure 1. Venn diagram and heat map depicting the number of statistically significant differentially expressed genes by experimental condition and across murine strains. The venn diagram in (A) depicts the number of genes that are differentially expressed in the surgical group versus sham. In (B) we show the number of differentially expressed genes across two strains, A/J and B6. (C) The heat map shows all differentially expressed genes between strains. (D) A heat map which shows the top 53 significantly regulated genes across two strains. For both heat maps, red = upregulated genes; green = downregulated genes.

Table 1. Differentially expressed genes with FDR < 0.05.			
	Total	Up	Down
A/J CBDL versus sham	582	404	178
B6 CBDL versus sham	137	76	61
Sham A/J versus B6	766	276	490
CBDL A/J versus B6	882	291	591

(Fig. 5), we performed a FITC-dextran permeability assay on Cdx2-IEC cells alone, Cdx2-IEC cells exposed to calcium-free media, Cdx2-IEC cells exposed to control siRNA, and Cdx2-IEC cells exposed to two different concentrations of MUP-1 siRNA (Fig. 6). As expected, cells exposed to calcium-free media resulted in a marked increase in cell permeability compared to Cdx2-IEC cells

in control media (**P* < 0.04). Cells treated with Control siRNA at 80 nmol/L and MUP-1 siRNA at 40 nmol/L concentrations were similar to untreated cells; whereas, cells treated with MUP-1 siRNA at 60 nmol/L concentration had significantly increased cell permeability compared to Cdx2-IEC cells in control media (***P* < 0.0002). Indeed, permeability of cells treated with MUP-1 siRNA at 60 nmol/L concentration was similar to cells in calcium-free media.

Discussion

Cholestasis can arise from a multitude of conditions in both the adult and pediatric population. In broad terms, cholestasis may result from biliary tract obstruction or hepatic parenchymal disease. Causes of biliary

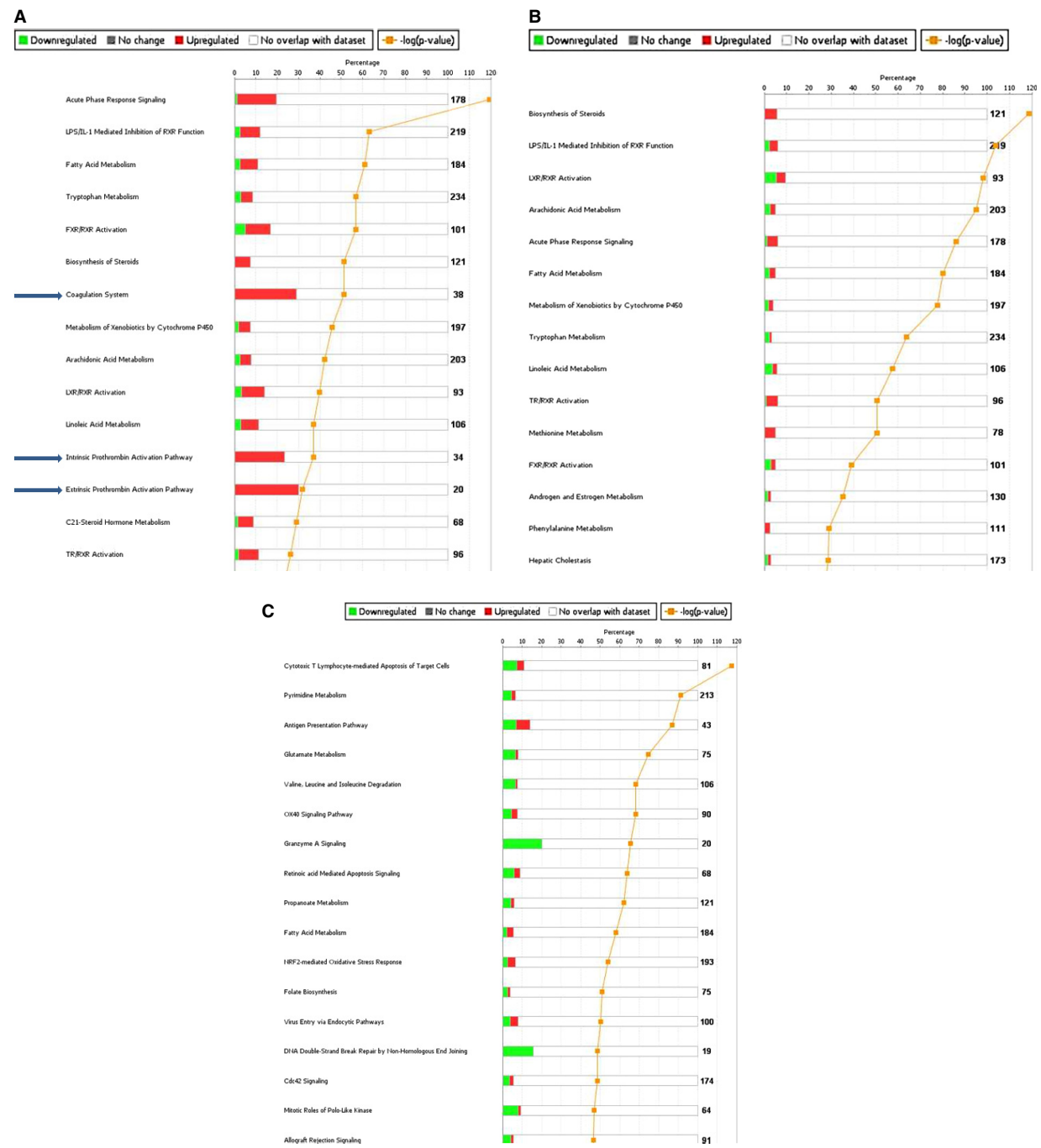


Figure 2. Significantly enriched canonical signaling pathways from differentially expressed gene sets. As denoted by the blue arrows in (A), coagulation pathways were highly upregulated in CBDL AJ mice compared with sham. In contrast, coagulation pathways were not significantly regulated in B6 CBDL versus sham (B). In (C), we show that there are a number of signaling pathways that are differentially regulated in AJ CBDL compared with B6 CBDL, demonstrating differential pathway activation in CBDL across these two inbred strains of mice.

tract obstruction in the adult include pancreatic carcinoma, duodenal carcinoma and cholangiocarcinoma, benign biliary strictures, and choledochal cyst; whereas, biliary atresia and choledochal cyst are seen in infants

and children. Causes of hepatic parenchymal disease in both age groups include hepatitis, total parenteral nutrition, sepsis, and other more rare cholestatic syndromes. In the neonatal population, cholestasis is commonly

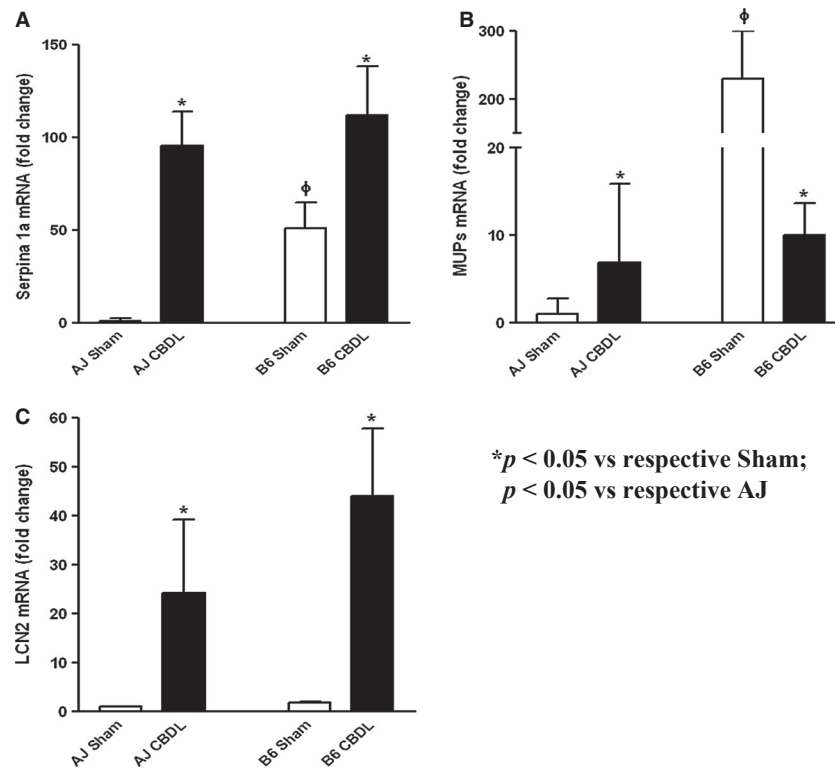


Figure 3. Serpina 1a, MUPs, and LCN2 gene expression changes determined by qPCR are consistent with microarray findings. (A) demonstrates a marked increase in Serpina 1a mRNA following CBDL in both strains. Also, there is a strain difference with increased Serpina 1a mRNA expression in B6 as compared to A/J mice. (B) demonstrates marked strain differences in MUP mRNA expression in the sham animals with disparate responses to CBDL. A/J sham MUP mRNA expression is low and expression increases following CBDL; whereas, in the B6 strain, MUP mRNA expression is very high in the sham group but falls in the CBDL group. (C) shows low expression of LCN2 mRNA in sham animals with marked increases following CBDL in both strains.

associated with a variety of intestinal pathologies, including necrotizing enterocolitis, intestinal atresias, midgut volvulus, gastroschisis, and Hirschsprung disease. In these conditions, a baby may not be able to tolerate much or any nutrition enterally. Total parenteral (intravenous) nutrition is required. As mentioned earlier, this type of nutrition causes cholestasis and the lack of enteral nutrition worsens the cholestasis; whereas, initiation of enteral nutrition and discontinuation of parenteral nutrition result in improvement of cholestatic liver dysfunction (Javid et al. 2005).

The goal of this study was to use microarray technology to generate candidate genes from both existing and novel pathways which play a role in the development of intestinal injury following cholestasis as modeled by CBDL. Using two different inbred strains of mice, A/J and C57Bl/6J, the design of this study had the benefit of not only discovering strain-independent but also strain-dependent changes in intestinal gene expression following cholestasis. More than 500 genes were increased by more than 2.0-fold following CBDL, and the following were

identified as promising candidate genes for further study: MUPs, Serpina1a, and LCN-2.

Major urinary proteins (MUPs) comprise the lipocalin superfamily of lipophilic ligand carriers which, until recently, were thought to participate exclusively in pheromone function. In a seminal article from 2009, MUP1 was shown to be a regulator for glucose and lipid metabolism, in addition to its action as a pheromone ligand to mediate chemical signaling in mice (Zhou et al. 2009). MUP production is known to be increased by testosterone, thyroid hormone, and growth hormone (GH) (Kuhn et al. 1984). The latter hormone is well known to play a significant role in intestinal healing following injury. Increased growth of the small bowel mucosa has been demonstrated in mice overexpressing bovine growth hormone (Ulshen et al. 1993). Moreover, recombinant growth hormone significantly attenuated intestinal mucosal injuries and bacterial translocation in septic rats (Yi et al. 2007), possibly through a mechanism involving the rhGH inhibition of apoptosis of intestinal mucosa cells. Endotoxemia was also reduced after GH administration in jaundiced rats (Scopa

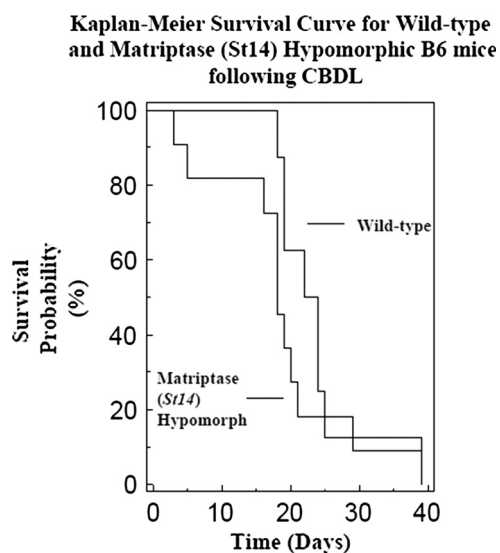


Figure 4. Kaplan–Meier survival curve for matriptase hypomorphic B6 and wild-type B6 mice following CBDL. The early trend toward increased mortality in the matriptase hypomorphic B6 mice is not statistically significant.

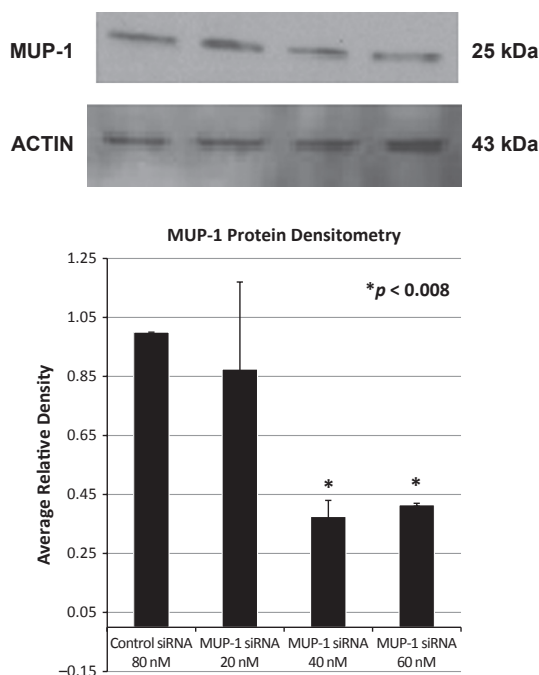


Figure 5. Western blot demonstrating silencing of MUP-1. Following their sixth passage, Cdx2-IEC cells were transfected with either MUP-1 siRNA (Thermo Scientific, Inc.) or Acell Control Non-Targeting siRNA (Thermo Scientific, Inc.). Western blot analysis was performed using MUP (F-3) mouse monoclonal antibody (Santa Cruz Biotechnology, Inc.).

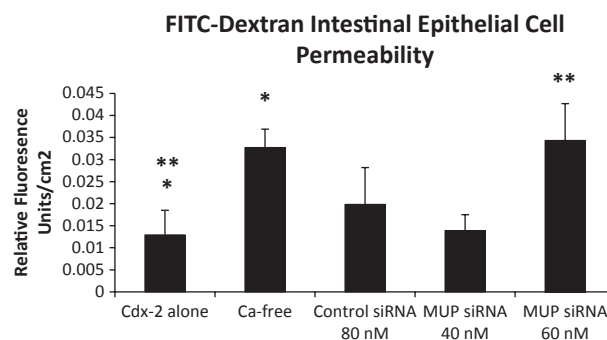


Figure 6. FITC-dextran permeability assay in Cdx2-IEC cells. Cells exposed to calcium-free (Ca-free) media resulted in a marked increase in cell permeability compared to Cdx2-IEC cells in control media ($*P < 0.04$). Cells treated with Control siRNA at 80 nmol/L and MUP-1 siRNA at 40 nmol/L concentrations were similar to untreated cells; whereas, cells treated with MUP-1 siRNA at 60 nmol/L concentration had significantly increased cell permeability compared to Cdx2-IEC cells in control media ($**P < 0.0002$). Indeed, permeability of cells treated with MUP-1 siRNA at 60 nmol/L concentration was similar to cells in calcium-free media.

et al. 2000). Some insight into the mechanism(s) by which GH exerts its effects have been elucidated in animal models. Prophylactic treatment with growth hormone promoted IgA secretion by B lymphocytes in the plasma and in the intestine in stressed postoperative rats (Ding et al. 2004). Similar effects have been seen in patients. GH was found to attenuate the depression in cellular immunity following surgical stress in a randomized, double-blind, controlled trial of 20 patients undergoing abdominal surgery (Liu et al. 2003). In addition, GH contributes to intestinal adaptation and has been documented to enable both adult and pediatric short gut syndrome patients to graduate from total parenteral nutrition (TPN) supplementation (Byrne et al. 1995; Velasco et al. 1999; Weiming et al. 2004). Growth hormone was also shown to reduce the increase in intestinal permeability seen following abdominal surgery (Liu et al. 2003). Consequently, when our microarray analysis demonstrated MUPs 1, 2, 3, 4, 7, 11, and 20 to be significantly increased following CBDL, we sought to explore this possible mechanism further. qPCR validated the microarray results and demonstrated a >200-fold increase in MUP expression in B6 sham mice compared to A/J sham mice. Most interestingly, the two strains of mice had different responses to CBDL. MUP expression increased >5-fold in A/J mice following CBDL; however, MUP expression in B6 mice decreased greatly following CBDL, such that there was no significant difference between two strains following CBDL. We speculate that GH rises in A/J mice following CBDL to increase MUP expression which, in turn, leads to increased intestinal resistance, strengthens the intestinal

barrier, and helps limit injury; whereas, in B6 mice, GH reserves and MUP expression have been depleted and simply cannot keep up with the injury. Further work is needed to clarify this.

We documented baseline expression of MUP-1 in intestinal epithelial cells. Following transfection of these cells with MUP-1 siRNA at 60 nmol/L concentration, we noticed a marked increase in cell permeability. This finding implicates increased MUP expression leading to increased intestinal resistance as a mechanism potentially responsible for the beneficial effects of growth hormone therapy.

Serpina1a is a gene on Chromosome 14 that encodes alpha-1 antitrypsin, which is a type of serine protease inhibitor, serpin. Our microarray analysis demonstrated a markedly elevated level of Serpina1a gene expression in the B6 sham mice, as well as dramatic increases in Serpina1a gene expression following CBDL in both strains. qPCR confirmed these findings. B6 sham mice had approximately 50-fold increased levels of expression compared to A/J sham mice. Furthermore, both strains exhibited approximately 100-fold increased levels of expression following CBDL when compared to the A/J sham mice.

A novel mechanism was suggested by the work of Bacher et al. (1992). They found that in gastrointestinal cell lines, the formation of tight junctions involves cellular proteases which are susceptible to protease inhibitors. Moreover, the recent work by Buzza and colleagues (2010) showing that Matriptase, a membrane-type serine protease-1, regulated epithelial barrier formation and permeability in the intestine intrigued us. Using matriptase (*St14*) hypomorphic mice which express less than 1% of the gene product, Buzza and colleagues (2010) demonstrated these mice to have a leaky intestinal barrier with decreased TEER and increased paracellular permeability. This raised the hypothesis that matriptase (*St14*) hypomorphic mice would have a higher mortality following CBDL than wild-type B6 mice. The increased expression of Serpina1a, coupled with the decreased intestinal resistance that we had found following CBDL, suggested to us that matriptase (*St14*) hypomorphic mice with decreased intestinal resistance and leaky tight junctions would not tolerate CBDL and the resultant further inhibition of serine protease-1 as well as the wild-type B6 mice. To our surprise, we did not find a striking effect on mortality. This might be explained in part by the work of Beliveau et al. (2009) which showed that under in vitro conditions, Serpina1a was an impotent inhibitor of matriptase compared to other serpins, such as antithrombin III. Antithrombin III may very well inhibit matriptase in vivo; however, further experiments would be necessary to confirm this. Whether antithrombin III increases mortality in matriptase hypomorphic mice following CBDL might be confounded by the known salutary effects of antithrombin

III in sepsis, including the attenuation of both hepatocyte apoptosis (Huang et al. 2010) and endotoxemia-induced healing impairment in the colon (Diller et al. 2009), as well as preserved mucosal thickness and villus height following CBDL (Caglikulekci et al. 2004). Nevertheless, our results suggest that matriptase does not play a significant role in the mortality following CBDL.

A potential mechanism behind the role of Serpina1a in the cholestatic intestine might be akin to that seen in studies of lung inflammation. Alpha-1 antitrypsin inhibits the enzyme, neutrophil elastase, which is released from neutrophils and macrophages during inflammation; neutrophil elastase destroys both bacteria and host tissue. Neutrophil elastase has also been shown to play a significant role in the pathogenesis of lung injury in pulmonary fibrosis (Yamanouchi et al. 1998). Moreover, alpha-1 antitrypsin was shown to induce hepatocyte growth factor (HGF) production by human lung fibroblasts and function as an anti-inflammatory and regenerative factor in addition to its role in protease inhibition (Kikuchi et al. 2000). HGF has previously been shown to increase intestinal epithelial cell mass and function in vivo (Kato et al. 1997) and also stimulate DNA content and protein content beyond the normal adaptive response following massive small intestinal resection (Kato et al. 1998). Our data suggest that increased expression of Serpina1a would increase HGF and provide a therapeutic approach to limit the intestinal injury following cholestasis, analogous to a recent study, in which alpha-1 antitrypsin therapy was shown to decrease intestinal permeability and ameliorate acute colitis and chronic ileitis in a murine model (Collins et al. 2013).

Lipocalin-2 is an iron-sequestering protein in the anti-bacterial innate immune response. Upon encountering invading bacteria, the Toll-like receptor 4 (TLR4) on immune cells stimulates the transcription, translation, and secretion of lipocalin-2 (Flo et al. 2004). It binds to siderophores secreted by pathogenic bacteria, including enterochelin secreted by *E. coli*, and prevents bacterial iron uptake (Flo et al. 2004). LCN2^{-/-} mice have decreased survival following *E. coli* infection compared to wild-type mice (Berger et al. 2006). Neutrophils isolated from LCN2^{-/-} mice showed significantly less bacteriostatic activity compared with wild-type controls. The bacteriostatic property of the wild-type neutrophils was abolished by the addition of exogenous iron, indicating that the main function of lipocalin-2 is to limit this essential element (Berger et al. 2006). Similarly, lipocalin-2 resistance confers an advantage to *Salmonella enterica* serotype Typhimurium for growth and survival in the inflamed intestine (Rafatellu et al. 2009). Our microarray analysis demonstrated significant increases in LCN2 following CBDL. qPCR confirmed this finding and is consistent with a strain-independent response to CBDL. LCN2

expression increased more than 20-fold and 40-fold, respectively, in A/J and B6 mice following CBDL. Increased LCN2 gene expression in the intestine following CBDL appears to be a mechanism whereby the host limits injury and mortality. This appears analogous to the increase in LCN2 gene expression coincident with an increase in epithelial cell apoptosis associated with intestinal adaptation following massive small bowel resection (Wildhaber et al. 2003). This is in agreement with earlier work by Devireddy et al. (2001) demonstrating lipocalin-2 to induce apoptosis in hematopoietic cells by an autocrine pathway. Thus, lipocalin-2 is a regulatory factor of intestinal growth.

In summary, our study has generated a resource of candidate genes for intestinal injury secondary to cholestasis. For *Serpina1a*, MUPs, and LCN2, some of the genes whose expression was most dramatically affected by CBDL, we confirmed the microarray results with qPCR. Novel mechanisms implicated by our results involve the growth hormone pathway, the acute phase response, and the innate immune response. More research is needed to further define these mechanisms; however, future therapeutic strategies might include: overexpression of *Serpina1a* and increased levels of HGF, upregulation of the GH pathway and increased MUP expression, and increased LCN2 expression to limit intestinal injury following cholestasis.

Conflict of Interest

None declared.

References

- Alaish, S. M., M. Torres, M. Ferlito, C. Sun, and A. De Maio. 2005. The severity of cholestatic injury is modulated by the genetic background. *Shock* 24:412–416.
- Alaish, S. M., A. D. Smith, J. Timmons, J. Greenspon, D. Eyvazzadeh, E. Murphy, et al. 2013. Gut microbiota, tight junction protein expression, intestinal resistance, bacterial translocation and mortality following cholestasis depend on the genetic background of the host. *Gut Microbes* 4:1–14.
- Bacher, A., K. Griehl, S. Mackamul, R. Mitreiter, H. Muckter, and Y. Ben-Shaul. 1992. Protease inhibitors suppress the formation of tight junctions in gastrointestinal cell lines. *Exp. Cell Res.* 200:97–104.
- Beliveau, F., A. Desilets, and R. Leduc. 2009. Probing the substrate specificities of matriptase, matriptase-2, hepsin, and DESC1 with internally quenched fluorescent peptides. *FEBS J.* 276:2213–2226.
- Berger, T., A. Togawa, G. S. Duncan, A. J. Elia, A. You-Ten, A. Wakeham, et al. 2006. Lipocalin-2-deficient mice exhibit increased sensitivity to *Escherichia coli* infection but not ischemia-reperfusion injury. *PNAS* 103:1834–1839.
- Bruewer, M., A. Luegering, T. Kucharzik, C. A. Parkos, J. L. Madara, A. M. Hopkins, et al. 2003. Proinflammatory cytokines disrupt epithelial barrier function by apoptosis-independent mechanisms. *J. Immunol.* 171:6164–6172.
- Buzza, M. S., S. Netzel-Arnett, T. Shea-Donahue, A. Zhao, C.-Y. Lin, K. List, et al. 2010. Membrane-anchored serine protease matriptase regulates epithelial barrier formation and permeability in the intestine. *PNAS* 107:4200–4205.
- Byrne, T. A., R. L. Persinger, L. S. Young, T. R. Ziegler, and D. W. Wilmore. 1995. A new treatment for patients with short-bowel syndrome: growth hormone, glutamine and a modified diet. *Ann. Surg.* 222:243–254.
- Caglikulekci, M., M. Dirlik, O. Scatton, I. Cinel, I. Ozer, L. Cinel, et al. 2004. Effect of antithrombin-III (AT-III) on intestinal epithelium changes related to obstructive icterus: experimental study in rats. *Ann. Chir.* 129:273–277.
- Campillo, B., P. Pernet, P. N. Bories, J. P. Richardet, M. Devanlay, and C. Aussel. 1999. Intestinal permeability in liver cirrhosis: relationship with severe septic complications. *Eur. J. Gastroenterol. Hepatol.* 11:755–759.
- Clayburgh, D. R., L. Shen, and J. R. Turner. 2004. A porous defense: the leaky epithelial barrier in intestinal disease. *Lab. Invest.* 84:282–291.
- Collins, C. B., C. M. Aherne, S. F. Ehrentraut, M. E. Gerich, E. N. McNamee, M. C. McManus, et al. 2013. Alpha-1-antitrypsin therapy ameliorates acute colitis and chronic murine ileitis. *Inflamm. Bowel Dis.* 19:1964–1973.
- Devireddy, L. R., J. G. Teodoro, F. A. Richard, and M. R. Green. 2001. Induction of apoptosis by a secreted lipocalin that is transcriptionally regulated by IL-3 deprivation. *Science* 293:829–834.
- Diller, R., U. Stratmann, E. Minin, C. von Eiff, G. Baumer, H. Huismans, et al. 2009. ATIII attenuates endotoxemia induced healing impairment in the colon. *J. Surg. Res.* 157:4–13.
- Ding, L., J.-S. Li, Y.-S. Li, F. N. Liu, and L. Tan. 2004. Prophylactic treatment with growth hormone improves intestinal barrier function and alleviates bacterial translocation in stressed rats. *Chin. Med. J.* 117:264–269.
- Dorsey, S. G., C. C. Leitch, C. L. Renn, S. Lessans, B. A. Smith, X. M. Wang, et al. 2009. Genome-wide screen identifies drug-induced regulation of the gene giant axonal neuropathy (Gan) in a mouse model of antiretroviral-induced painful peripheral neuropathy. *Biol. Res. Nurs.* 11:7–16.
- El Asmar, R., P. Panigrahi, P. Bamford, I. Berti, T. Not, G. V. Coppa, et al. 2002. Host-dependent zonulin secretion causes the impairment of the small intestine barrier function after bacterial exposure. *Gastroenterology* 123:1607–1615.
- Flo, T. H., K. D. Smith, S. Sato, D. J. Rodriguez, M. A. Holmes, R. K. Strong, et al. 2004. Lipocalin 2

- mediates an innate immune response to bacterial infection by sequestering iron. *Nature* 432:917–921.
- Frances, R., S. Benlloch, P. Zapater, J. M. Gonzalez, B. Lozano, C. Munoz, et al. 2004. A sequential study of serum bacterial DNA in patients with advanced cirrhosis and ascites. *Hepatology* 39:484–491.
- Georgiev, P., W. Jochum, S. Heinrich, J. H. Jang, A. Nocito, F. Dahm, et al. 2008. Characterization of time-related changes after experimental bile duct ligation. *Br. J. Surg.* 95:646–656.
- Huang, C.-Y., S.-M. Sheen-Chen, H.-T. Ho, R. P. Tang, and H. L. Eng. 2010. Antithrombin-III attenuates hepatocyte apoptosis in bile duct ligated rat: a striking cellular change. *Surg. Innov.* 17:132–135.
- Javid, P. J., S. Collier, D. Richardson, J. Iglesias, K. Gura, C. Lo, et al. 2005. The role of enteral nutrition in the reversal of parenteral-nutrition-associated liver dysfunction in infants. *J. Pediatr. Surg.* 40:1015–1018.
- Kato, Y., D. Yu, J. R. Lukish, and M. Z. Schwartz. 1997. Hepatocyte growth factor enhances intestinal mucosal cell function and mass in vivo. *J. Pediatr. Surg.* 32:991–994.
- Kato, Y., D. Yu, and M. Z. Schwartz. 1998. Enhancement of intestinal adaptation by hepatocyte growth factor. *J. Pediatr. Surg.* 33:235–239.
- Kikuchi, T., T. Abe, M. Yaekashiwa, Y. Tominaga, H. Mitsuhashi, K. Satoh, et al. 2000. Secretory leukoprotease inhibitor augments hepatocyte growth factor production in human lung fibroblasts. *Am. J. Respir. Cell Mol. Biol.* 23:364–370.
- Kuhn, N. J., M. Woodworth-Gutai, K. W. Gross, and W. A. Held. 1984. Subfamilies of the mouse major urinary protein (MUP) multi-gene family: sequence analysis of cDNA clones and differential regulation in the liver. *Nucleic Acids Res.* 12:6073–6090.
- List, K., B. Currie, T. C. Scharschmidt, R. Szabo, J. Shireman, A. Molinolo, et al. 2007. Autosomal ichthyosis with hypotrichosis syndrome displays low matriptase proteolytic activity and is phenocopied in ST14 hypomorphic mice. *J. Biol. Chem.* 282:36714–36723.
- Liu, W., Z. Jiang, X. Wang, H. Shu, W. Cui, and D. W. Wilmore. 2003. Impact of perioperative treatment of recombinant human growth hormone on cell immune function and intestinal barrier function: randomized, double-blind, controlled trial. *World J. Surg.* 27:412–415.
- Madara, J. L., and J. Stafford. 1989. Interferon-gamma directly affects barrier function of cultured intestinal epithelial monolayers. *J. Clin. Invest.* 83:724–727.
- Marano, C. W., S. A. Lewis, L. A. Garulacan, A. P. Soler, and J. M. Mullin. 1998. Tumor necrosis factor- α increases sodium and chloride conductance across the tight junction of CACO-2 BBE, a human intestinal epithelial cell line. *J. Membr. Biol.* 161:263–274.
- Pascual, S., J. Such, A. Esteban, P. Zapater, J. A. Casellas, J. R. Aparicio, et al. 2003. Intestinal permeability is increased in patients with advanced cirrhosis. *Hepatology* 50:1482–1486.
- Rafatellu, M., M. D. George, Y. Akiyama, M. J. Hornsby, S. P. Nuccio, T. A. Paixao, et al. 2009. Lipocalin-2 resistance confers an advantage to *Salmonella enterica* serotype Typhimurium for growth and survival in the inflamed intestine. *Cell Host Microbe* 5:476–486.
- Rao, J. N., O. Platoshyn, V. A. Golovina, L. Liu, T. Zou, B. S. Marasa, et al. 2006. TRPC1 functions as a store-operated Ca^{2+} channel in intestinal epithelial cells and regulates early mucosal restitution after wounding. *Am. J. Physiol. Gastrointest. Liver Physiol.* 290:G782–G792.
- Scopa, C. D., S. Koureleas, A. C. Tsamandas, I. Spiliopoulou, T. Alexandrides, K. S. Filos, et al. 2000. Beneficial effects of growth hormone and insulin-like growth factor I on intestinal bacterial translocation, endotoxemia, and apoptosis in experimentally jaundiced rats. *J. Am. Coll. Surg.* 190:423–431.
- Ulshen, M. H., R. H. Dowling, C. R. Fuller, E. M. Zimmermann, and P. K. Lund. 1993. Enhanced growth of small bowel in transgenic mice overexpressing bovine growth hormone. *Gastroenterology* 104:973–980.
- Velasco, B., L. Lassaletta, R. Gracia, and J. A. Tovar. 1999. Intestinal lengthening and growth hormone in extreme short bowel syndrome: a case report. *J. Pediatr. Surg.* 34:1423–1424.
- Weiming, Z., L. Ning, and L. Jieshou. 2004. Effect of recombinant human growth hormone and enteral nutrition on short bowel syndrome. *J. Parenter. Enteral Nutr.* 28:377–381.
- Wildhaber, B. E., H. Yang, A. G. Coran, and D. H. Teitelbaum. 2003. Gene alteration of intestinal intraepithelial lymphocytes in response to massive small bowel resection. *Pediatr. Surg. Int.* 19:310–315.
- Yamanouchi, H., J. Fujita, S. Hojo, T. Yoshinouchi, T. Kamei, I. Yamadori, et al. 1998. Neutrophil elastase: α -1-proteinase inhibitor complex in serum and bronchoalveolar lavage fluid in patients with pulmonary fibrosis. *Eur. Respir. J.* 11:120–125.
- Yi, C., Y. Cao, S. R. Wang, Y. Z. Xu, H. Huang, Y. X. Cui, et al. 2007. Beneficial effect of recombinant human growth hormone on the intestinal mucosa barrier of septic rats. *Braz. J. Med. Biol. Res.* 40:41–48.
- Youakim, A., and M. Ahdieh. 1999. Interferon-gamma decreases barrier function in T84 cells by reducing ZO-1 levels and disrupting apical actin. *Am. J. Physiol.* 276: G1279–G1288.
- Zhou, Y., L. Jiang, and L. Rui. 2009. Identification of MUP1 as a regulator for glucose and lipid metabolism in mice. *J. Biol. Chem.* 284:11152–11159.

Appendix

Table A1. List of all differentially expressed genes.

Probe set ID	Gene accession	Gene symbol	Gene description	Cytoband	AJ CBDL vs sham FC	AJ CBDL vs sham FDR	B6 CBDL vs sham FC	B6 CBDL vs sham FDR
10566477	NM_017371	Hpx	hemopexin	7 F1	37.4012	1.00E-04	4.7408	0.0435
10581605	NM_017370	Hp	haptoglobin	8 D3 8 55.0 cM	34.152	3.00E-04	6.662	0.0445
10505438	NM_008768	Orm1	orosomucoid 1	4 B3 4 31.4 cM	18.2062	2.00E-04	4.3826	0.0404
10414192	NM_133653	Mat1a	methionine adenosyltransferase I, alpha	14 C1	17.981	0.001	7.268	0.0306
10511886	NM_016668 // NM_016668	Bhmt // Bhmt	betaine-homocysteine methyltransferase // betaine-homocysteine methyltransferase	13 D1 // 13 D1	17.9485	0.0014	10.4211	0.0197
10457114	NM_016668	Bhmt	betaine-homocysteine methyltransferase	13 D1	15.6549	5.00E-04	8.3998	0.0109
10578352	NM_145594	Fgl1	fibrinogen-like protein 1	8 A4	13.8891	1.00E-04	4.1148	0.0178
10575349	NM_146214	Tat	tyrosine aminotransferase	8 D3	12.4752	3.00E-04	4.323	0.0294
10449452	NM_010220	Fkbp5	FK506 binding protein 5	17 A3.3 17 13.0 cM	11.8521	0.0015	6.359	0.0294
10490989	NM_001042611	Cp	ceruloplasmin	3 D	11.1162	0	3.3852	0.0109
10481627	NM_008491	Lcn2	lipocalin 2	2 A3 2 27.0 cM	9.7186	8.00E-04	8.0914	0.0098
10360328	NM_011318	Apcs	serum amyloid P-component	1 H3 1 94.2 cM	9.2166	0	3.1253	0.0123
10451953	NM_029796	Lrg1	leucine-rich alpha-2-glycoprotein 1	17 D 17 10.0 cM	6.9919	6.00E-04	5.0051	0.0109
10574023	NM_008630	Mt2	metallothionein 2	8 C5 8 45.0 cM	6.9697	0.0206	8.4549	0.0307
10515187	NM_007822	Cyp4a14	cytochrome P450, family 4, subfamily a, polypeptide 14	4 D1 4 49.5 cM	4.6609	0.0378	9.8282	0.015
10418434	NM_008407	Itih3	inter-alpha trypsin inhibitor, heavy chain 3	14 A2-C1	4.2071	9.00E-04	4.0594	0.0078
10543017	NM_013743	Pdk4	pyruvate dehydrogenase kinase, isoenzyme 4	6 A1 6 0.63 cM	3.5193	0.0145	3.492	0.0368
10503520	NM_015767	Ttpa	tocopherol (alpha) transfer protein	4 A3 4 22.7 cM	3.3338	0.003	2.5756	0.0354
10492748	NM_010196	Fga	fibrinogen alpha chain	3 F1 3 44.8 cM	3.1077	0.0013	2.2512	0.0307
10496727	NM_026993	Ddah1	dimethylarginine dimethylaminohydrolase 1	3 H3	3.0694	0.001	2.967	0.0098
10583732	NM_010700	Ldlr	low density lipoprotein receptor	9 A3 9 5.0 cM	3.0527	0	2.0755	0.0024
10507177	NM_001100181	Cyp4a32	cytochrome P450, family 4, subfamily a, polypeptide 32	4 D1	2.7853	0.0347	3.3932	0.0344
10527920	NM_020010	Cyp51	cytochrome P450, family 51	5 A2 5 1.2 cM	2.7708	0.001	2.3088	0.015

Table A1. Continued.

Probe set ID	Gene accession	Gene symbol	Gene description	Cytoband	AJ CBDL vs sham FC	AJ CBDL vs sham FDR	B6 CBDL vs sham FC	B6 CBDL vs sham FDR
10362073	NM_001161845	Sgk1	serum/glucocorticoid regulated kinase 1	10 A3	2.7412	0.0073	3.4689	0.0109
10379153	NM_009657	Aldoc	aldolase C, fructose-bisphosphate	11 B5 11 44.98 cM	2.699	0.0096	2.6246	0.0301
10420730	NM_010191	Fdft1	farnesyl diphosphate farnesyl transferase 1	14 D1 14 3.0 cM	2.6151	0.001	2.0228	0.0228
10515201	NM_007823	Cyp4b1	cytochrome P450, family 4, subfamily b, polypeptide 1	4 D1 4 49.5 cM	2.5614	0.001	1.7862	0.0445
10568001	NM_133670	Sult1a1	sulfotransferase family 1A, phenol-preferring, member 1	7 F3 7 4.0 cM	2.5199	1.00E-04	1.7899	0.0109
10520362	NM_153526	Insig1	insulin induced gene 1	5 B1	2.4631	0.0014	1.836	0.0451
10412909	NM_010191	Fdft1	farnesyl diphosphate farnesyl transferase 1	14 D1 14 3.0 cM	2.4306	6.00E-04	2.072	0.0109
10424349	NM_009270	Sqle	squalene epoxidase	15 D1	2.3683	0.0023	1.9609	0.0307
10478048	NM_008489	Lbp	lipopolysaccharide binding protein	2 H1 2 83.0 cM	2.3404	6.00E-04	1.8161	0.0194
10499483	NM_134469	Fdps	farnesyl diphosphate synthetase	3 F1 3 42.6 cM	2.2316	0.0044	2.2171	0.017
10412466	NM_145942	Hmgcs1	3-hydroxy-3-methylglutaryl-Coenzyme A synthase 1	—	2.213	0.0012	1.7749	0.0294
10364194	NM_146006	Lss	lanosterol synthase	10 C1 10 41.1 cM	2.1256	0.0051	1.9021	0.0346
10378793	NM_025655	Tmigd1	transmembrane and immunoglobulin domain containing 1	11 B5	2.0643	0.0316	3.0221	0.0109
10365830	—	—	—	—	2.0533	0.0032	1.9576	0.0178
10542470	NM_019946	Mgst1	microsomal glutathione S-transferase 1	6 G1	1.9951	0.0124	1.9203	0.0416
10506571	NM_053272	Dhcr24	24-dehydrocholesterol reductase	4 C7	1.8836	0.0014	1.8709	0.0109
10450242	NM_009780	C4b	complement component 4B (Chido blood group)	17 B1 17 18.8 cM	1.8607	0.0124	1.849	0.0333
10585942	NM_001033498	Gramd2	GRAM domain containing 2	9 B	1.8264	0.0037	1.622	0.0375
10493548	NM_026784	Pmvk	phosphomevalonate kinase	3 F1	1.7852	0.0105	1.808	0.0273
10492964	NM_009690	Cd5l	CD5 antigen-like	3 F1	1.6284	0.0195	1.8539	0.0169
10524555	NM_023556	Mvk	mevalonate kinase	5 F 5 64.0 cM	1.6043	0.0144	1.63	0.0307
10600082	NM_010941	Nsdhl	NAD(P) dependent steroid dehydrogenase-like	X A7.3 X 28.87 cM	1.5727	0.009	1.7157	0.0116
10573626	NM_173866	Gpt2	glutamic pyruvate transaminase (alanine aminotransferase) 2	8 C3	1.5293	0.0438	1.6633	0.0425
10526630	NM_015799	Trfr2	transferrin receptor 2	5 G2	1.5175	0.0197	1.5238	0.0435
10456699	NM_177470	Acaa2	acetyl-Coenzyme A acyltransferase 2 (mitochondrial 3-oxoacyl-Coenzyme A thiolase)	18 E2 18 45.0 cM	1.5095	0.029	1.6537	0.0273

Table A1. Continued.

Probe set ID	Gene accession	Gene symbol	Gene description	Cytoband	AJ CBDL vs sham FC	AJ CBDL vs sham FDR	B6 CBDL vs sham FC	B6 CBDL vs sham FDR
10393970	NM_007988	Fasn	fatty acid synthase	11 E2 11 72.0 cM	1.4769	0.004	1.4846	0.015
10525893	NM_030210	Aacs	acetoacetyl-CoA synthetase	5 F	1.4673	0.0242	1.4896	0.0456
10425695	NM_033218	Srebf2	sterol regulatory element binding factor 2	15 E1	1.4633	0.0095	1.4826	0.0233
10569972	NM_026058	Lass4	LAG1 homolog, ceramide synthase 4	8 A1.2	1.4318	0.0145	1.5	0.0228
10570437	NM_025785	Fbxo25	F-box protein 25	8 A1.1	-1.3809	0.0356	-1.4953	0.0294
10447239	NM_026180	Abcg8	ATP-binding cassette, sub-family G (WHITE), member 8	17 E4 17 54.5 cM	-1.5584	0.013	-1.8003	0.0109
10425945	NM_010180	Fbln1	fibulin 1	15 E-F	-1.5672	0.013	-1.601	0.0287
10453318	NM_031884	Abcg5	ATP-binding cassette, sub-family G (WHITE), member 5	17 E4 17 54.5 cM	-1.6829	0.0069	-1.6878	0.0224
10390032	NM_153807	Acsf2	acyl-CoA synthetase family member 2	11 D	-1.8821	0.0041	-2.228	0.0078
10492426	NM_153807	Acsf2	acyl-CoA synthetase family member 2	11 D	-1.9567	0.0045	-2.1236	0.0109
10518674	NM_022020	Rbp7	retinol binding protein 7, cellular	4 E2	-2.0739	0.0021	-1.8152	0.0258
10462442	NM_001164724	Il33	interleukin 33	19 C2	-2.0935	0.0078	-1.9454	0.0354
10575833	NM_008290	Hsd17b2	hydroxysteroid (17-beta) dehydrogenase 2	8 E1	-2.2055	0.0025	-1.9459	0.026
10577655	NM_008324	Ido1	indoleamine 2,3-dioxygenase 1	8 A2	-2.4459	0.0461	-3.4593	0.0249
10463005	NM_028089	Cyp2c55	cytochrome P450, family 2, subfamily c, polypeptide 55	19 C3	-2.5559	0.0458	-14.6416	4.00E-04
10373334	NM_013786	Hsd17b6	hydroxysteroid (17-beta) dehydrogenase 6	10 D3	-2.6186	2.00E-04	-1.7122	0.0241
10502214	NM_027816	Cyp2u1	cytochrome P450, family 2, subfamily u, polypeptide 1	3 H1	-3.4307	1.00E-04	-1.6652	0.0425
10514912	NM_007860	Dio1	deiodinase, iodothyronine, type I	4 C7 4 48.7 cM	-4.5064	0.0012	-3.8938	0.0109
10480155	NM_001081084	Cubn	cubilin (intrinsic factor -cobalamin receptor)	2 A1 2 9.0 cM	-4.8123	3.00E-04	-2.7793	0.016
10585749	NM_009992	Cyp1a1	cytochrome P450, family 1, subfamily a, polypeptide 1	9 B 9 31.0 cM	-5.6507	0.001	-3.3135	0.0301
10513420	NM_001134675	Mup7	major urinary protein 7	4 B3 4	127.8618	0.001		
10513455	NM_008647	Mup2	major urinary protein 2	4 B3	126.9789	0.001		
10513437	NM_001164526	Mup11	major urinary protein 11	4 B3	117.1801	0.001		
10513428	NM_001045550	Mup2	major urinary protein 2	4 B3	113.5703	0.001		
10513472	NM_008647	Mup2	major urinary protein 2	4 B3	104.5563	0.001		
10513504	NM_001045550	Mup2	major urinary protein 2	4 B3	100.7876	0.001		

Table A1. Continued.

Probe set ID	Gene accession	Gene symbol	Gene description	Cytoband	AJ CBDL vs sham FC	AJ CBDL vs sham FDR	B6 CBDL vs sham FC	B6 CBDL vs sham FDR
10513497	NM_001045550	Mup2	major urinary protein 2	4 B3	94.2911	0.001		
10513521	NM_001012323	Mup20	major urinary protein 20	4 B3	93.1978	0.0021		
10513467	NM_001045550	Mup2	major urinary protein 2	4 B3	90.6275	0.001		
10513512	NM_001163011	Mup1	major urinary protein 1	4 B3 4 27.8 cM	73.9991	0.001		
10523062	NM_009654	Alb	albumin	5 E1 5 50.0 cM	61.2531	4.00E-04		
10434689	NM_013465	Ahsg	alpha-2-HS-glycoprotein	16 B1 16 15.0 cM	58.1197	3.00E-04		
10531149	NM_008096	Gc	group specific component	5 E1 5 44.0 cM	52.3423	1.00E-04		
10492735	NM_133862	Fgg	fibrinogen gamma chain	3 E3 3 41.3 cM	38.7526	1.00E-04		
10498981	NM_181849	Fgb	fibrinogen beta chain	3 E3 3 48.2 cM	38.2336	1.00E-04		
10402406	NM_009245	Serpina1c	serine (or cysteine) peptidase inhibitor, clade A, member 1C	12 E 12 51.0 cM	30.3389	3.00E-04		
10402399	NM_009243	Serpina1a	serine (or cysteine) peptidase inhibitor, clade A, member 1A	12 E 12 51.0 cM	23.9693	3.00E-04		
10558673	NM_021282	Cyp2e1	cytochrome P450, family 2, subfamily e, polypeptide 1	7 F5 7 68.4 cM	21.9342	0.0012		
10562169	NM_032541	Hamp	hepcidin antimicrobial peptide	7 B1 7 11.0 cM	21.1349	0.004		
10434719	NM_001102411	Knq1	kininogen 1	16 B1	19.6656	7.00E-04		
10402409	NM_009247	Serpina1e	serine (or cysteine) peptidase inhibitor, clade A, member 1E	12 E	18.9172	3.00E-04		
10548207	NM_007376	Pzp	pregnancy zone protein	6 F1-G3 6 62.0 cM	18.3515	3.00E-04		
10402390	NM_009244	Serpina1b	serine (or cysteine) peptidase inhibitor, clade A, member 1B	12 E 12 51.0 cM	15.5285	5.00E-04		
10498921	NM_019911	Tdo2	tryptophan 2,3-dioxygenase	3 E3	13.9226	0.0023		
10596148	NM_133977	Trf	transferrin	9 F1-F3 9 56.0 cM	13.3568	4.00E-04		
10382189	NM_013475	Apoh	apolipoprotein H	11 D 11 63.0 cM	13.1193	0.001		
10553274	NM_011314	Saa2	serum amyloid A 2	7 B4 7 23.5 cM	10.9174	0.015		
10541480	NR_027619	Mug-ps1	murinoglobulin, pseudogene 1	6 F1	10.2599	0.0013		
10496825	NM_009474	Uox	urate oxidase	3 H2 3 75.0 cM	10.1685	0.0046		
10497337	NM_009799	Car1	carbonic anhydrase 1	3 A1 3 10.5 cM	9.9909	0.0175		
10454192	NM_013697	Ttr	transthyretin	18 A2 18 7.0 cM	9.9844	0.0025		
10463037	NM_010003	Cyp2c39	cytochrome P450, family 2, subfamily c, polypeptide 39	19 C3	9.7038	1.00E-04		
10398060	NM_011458	Serpina3k	serine (or cysteine) peptidase inhibitor, clade A, member 3K	12 E 12 51.5 cM	9.5497	0.0042		
10541448	NR_027619	Mug-ps1	murinoglobulin, pseudogene 1	6 F1	9.4334	0.0027		
10541410	NM_008645	Mug1	murinoglobulin 1	6 F1	9.3764	0.001		
10379190	NM_011707	Vtn	vitronectin	11 B5 11 45.09 cM	8.9998	0.0014		
10431915	NM_027052	Slc38a4	solute carrier family 38, member 4	15 F1	8.9956	0.0027		
10351546	NM_013474	Apoa2	apolipoprotein A-II	1 H3 1 92.6 cM	8.8013	8.00E-04		

Table A1. Continued.

Probe set ID	Gene accession	Gene symbol	Gene description	Cytoband	AJ CBDL vs sham FC	AJ CBDL vs sham FDR	B6 CBDL vs sham FC	B6 CBDL vs sham FDR
10467410	NM_145499	Cyp2c70	cytochrome P450, family 2, subfamily c, polypeptide 70	19 C3	8.4844	0.0014		
10467319	NM_001159487	Rbp4	retinol binding protein 4, plasma	19 D1 19 38.0 cM	7.858	0.0021		
10542983	NM_011134	Pon1	paraoxonase 1	6 A2 6 0.5 cM	7.6708	0.021		
10560618	NM_007469	Apoc1	apolipoprotein C-I	7 A3 7 4.0 cM	7.6693	0.0065		
10398075	NM_009252	Serpina3n	serine (or cysteine) peptidase inhibitor, clade A, member 3N	12 F1	7.4314	0.0115		
10368343	NM_007482	Arg1	arginase, liver	10 A4	7.3671	9.00E-04		
10563611	NM_009117	Saa1	serum amyloid A 1	7 B4 7 23.5 cM	7.1769	0.0095		
10434709	NM_053176	Hrg	histidine-rich glycoprotein	16 B1 16 14.1 cM	7.0319	0.0028		
10513529	NM_001039544	Mup3	major urinary protein 3	4 B3	6.9857	0.0286		
10549154	BC151094	Gm766	predicted gene 766	6 G3	6.9004	0.0267		
10413615	NM_018746	Itih4	inter alpha-trypsin inhibitor, heavy chain 4	14 B 14 11.75 cM	6.7951	0.0012		
10441753	NM_008877	Plg	plasminogen	17 A1 17 7.3 cM	6.266	0.0022		
10401289	NM_001177561	Slc10a1	solute carrier family 10 (sodium/bile acid cotransporter family), member 1	12 D1 12 37.0 cM	6.0785	0.0028		
10485027	NM_010168	F2	coagulation factor II	2 E1 2 47.5 cM	6.048	0.0096		
10402394	NM_009246	Serpina1d	serine (or cysteine) peptidase inhibitor, clade A, member 1D	12 E 12 51.0 cM	6.0378	0.0135		
10363860	NM_025807	Slc16a9	solute carrier family 16 (monocarboxylic acid transporters), member 9	10 B5.3	5.8753	0.0065		
10434698	NM_021564	Fetub	fetuin beta	16 B 16 14.1 cM	5.7467	0.0098		
10580635	NM_053200	Ces3	carboxylesterase 3	8 C5	5.6566	0.0021		
10526712	NM_013478	Azgp1	alpha-2-glycoprotein 1, zinc	5 G2 5 78.0 cM	5.4824	0.0232		
10506125	NM_013913	Angptl3	angiopoietin-like 3	4 C6 4 48.0 cM	5.2732	0.0124		
10580624	NM_007954	Es1	esterase 1	8 C5 8 43.0 cM	5.1268	0.0355		
10513630	NM_007443	Ambp	alpha 1 microglobulin/bikunin	4 C1-C3 4 30.6 cM	5.1009	0.0025		
10351852	NM_007768	Crp	C-reactive protein, pentraxin-related	1 H3 1 94.2 cM	4.9882	0.0025		
10363541	NM_007494	Ass1	argininosuccinate synthetase 1	2 B 2 20.0 cM	4.9534	0.0057		
10480003	NM_010582	Itih2	inter-alpha trypsin inhibitor, heavy chain 2	2 A1 2 1.0 cM	4.9513	0.0059		
10542615	NM_020495	Slco1b2	solute carrier organic anion transporter family, member 1b2	6 G1 6 67.0 cM	4.89	0.0212		
10367221	NM_133997	Apof	apolipoprotein F	10 D3 10 73.0 cM	4.8785	0.0025		
10551287	NM_133657	Cyp2a12	cytochrome P450, family 2, subfamily a, polypeptide 12	7 A3	4.8046	0.0096		

Table A1. Continued.

Probe set ID	Gene accession	Gene symbol	Gene description	Cytoband	AJ CBDL vs sham FC	AJ CBDL vs sham FDR	B6 CBDL vs sham FC	B6 CBDL vs sham FDR
10494643	NM_008256	Hmgcs2	3-hydroxy-3-methylglutaryl-Coenzyme A synthase 2	3 F2.2 3 48.0 cM	4.5815	0.0144		
10563602	NM_011316	Saa4	serum amyloid A 4	7 B4 7 23.5 cM	4.5245	0.001		
10471154	NM_007494	Ass1	argininosuccinate synthetase 1	2 B 2 20.0 cM	4.4979	0.0069		
10357516	NM_007576	C4bp	complement component 4 binding protein	1 E4 1 67.6 cM	4.4217	0.001		
10416451	NM_019775	Cpb2	carboxypeptidase B2 (plasma)	14 D2	4.3546	0.0036		
10551293	NM_007817	Cyp2f2	cytochrome P450, family 2, subfamily f, polypeptide 2	7 A3	4.2794	0.0394		
10398069	NM_009253	Serpina3m	serine (or cysteine) peptidase inhibitor, clade A, member 3M	12 E	4.2775	0.0231		
10438681	NM_201375	Kng2	kininogen 2	16 B1	4.2464	0.0051		
10367215	NM_133996	Apon	apolipoprotein N	10 D3 10 76.0 cM	4.2277	0.0021		
10351015	NM_080844	Serpinc1	serine (or cysteine) peptidase inhibitor, clade C (antithrombin), member 1	1 H2.1 1 84.6 cM	4.1985	0.0034		
10403322	NM_030611	Akr1c6	aldo-keto reductase family 1, member C6	13 A2 13 8.0 cM	4.1493	0.0498		
10452316	NM_009778	C3	complement component 3	17 E1-E3 17 34.3 cM	4.1151	0.0339		
10596718	NM_023805	Slc38a3	solute carrier family 38, member 3	9 F1 9 63.0 cM	4.1024	0.0239		
10501555	NM_007446	Amy1	amylase 1, salivary	3 F3 3 50.0 cM	4.1021	0.0069		
10519497	NM_054098	Steap4	STEAP family member 4	5 A1	3.9917	0.0063		
10496001	NM_007686	Cfi	complement component factor i	3 G3 3 66.6 cM	3.9698	0.0014		
10475532	NM_021507	Sqrdl	sulfide quinone reductase-like (yeast)	2 F2	3.9595	0		
10593225	NM_001033324	Zbtb16	zinc finger and BTB domain containing 16	9 A5.3 9 23.0 cM	3.8909	0.018		
10458828	NM_033037	Cdo1	cysteine dioxygenase 1, cytosolic	18 C 18 23.0 cM	3.7452	0.0025		
10514763	NM_146148	C8a	complement component 8, alpha polypeptide	4 C6	3.7375	0.0096		
10358339	NM_009888	Cfh	complement component factor h	1 F 1 74.1 cM	3.6868	0.0032		
10514532	NM_010007	Cyp2j5	cytochrome P450, family 2, subfamily j, polypeptide 5	4 C5 4 46.5 cM	3.6645	0.0256		
10450038	NM_020581	Angptl4	angiopoietin-like 4	17 B1	3.5851	0.0062		
10511375	NM_007824	Cyp7a1	cytochrome P450, family 7, subfamily a, polypeptide 1	4 A1	3.5797	0.0076		
10423002	NM_207216	Ugt3a1	UDP glycosyltransferases 3 family, polypeptide A1	15 A1	3.5454	0.0345		

Table A1. Continued.

Probe set ID	Gene accession	Gene symbol	Gene description	Cytoband	AJ CBDL vs sham FC	AJ CBDL vs sham FDR	B6 CBDL vs sham FC	B6 CBDL vs sham FDR
10483410	NM_021022	Abcb11	ATP-binding cassette, sub-family B (MDR/TAP), member 11	2 C2 2 38.4 cM	3.4306	0.0445		
10447885	NM_153151	Acat3	acetyl-Coenzyme A acetyltransferase 3	17 A1 17 7.55 cM	3.3695	0.0023		
10537169	NM_009731	Akr1b7	aldo-keto reductase family 1, member B7	6 B1 6 14.0 cM	3.3685	0.0032		
10395273	BC052902	Gdap10	ganglioside-induced differentiation-associated -protein 10	12 A3	3.3561	0.0043		
10503502	NM_015767	Ttpa	tocopherol (alpha) transfer protein	4 A3 4 22.7 cM	3.2169	0.0089		
10585015	NM_080434	Apoa5	apolipoprotein A-V	9 B	3.2153	0.0026		
10581388	NM_008490	Lcat	lecithin cholesterol acyltransferase	8 D3 8 53.0 cM	3.2103	0.0014		
10482004	BC094504	Al182371	expressed sequence Al182371	2 B	3.1837	0.0281		
10574027	NM_013602	Mt1	metallothionein 1	8 C5 8 45.0 cM	3.1654	0.0374		
10379736	NM_183249	1100001G20Rik	RIKEN cDNA 1100001G20 gene	11 C	3.1049	0.0151		
10420899	NM_178747	Gulo	gulonolactone (L-) oxidase	14 D1	3.0186	0.0345		
10435626	NM_013547	Hgd	homogentisate 1, 2-dioxygenase	16 B3 16 27.3 cM	2.9656	0.0296		
10345065	NM_001077353	Gsta3	glutathione S-transferase, alpha 3	1 A4 1 15.0 cM	2.9309	0.0145		
10356145	NM_030556	Slc19a3	solute carrier family 19 (sodium/hydrogen exchanger), member 3	1 C5 1 51.0 cM	2.9123	0.0301		
10533612	NM_008277	Hpd	4-hydroxyphenylpyruvic acid dioxygenase	5 F 5 67.0 cM	2.8602	0.0373		
10451451	NM_010321	Gnmt	glycine N-methyltransferase	17 C 17 10.0 cM	2.8319	0.0461		
10543333	NM_013930	Aass	aminoadipate-semialdehyde synthase	6 A3.1 6 4.5 cM	2.8069	0.0115		
10596166	NM_027918	1300017J02Rik	RIKEN cDNA 1300017J02 gene	9 F1	2.7756	0.0308		
10406646	NM_028772	Dmgdh	dimethylglycine dehydrogenase precursor	13 C3	2.7336	0.0244		
10500547	NM_153193	Hsd3b2	hydroxy-delta-5-steroid dehydrogenase, 3 beta- and steroid delta-isomerase 2	3 F2.2 3 49.1 cM	2.6399	0.0032		
10570717	NM_001177522	Gm14850	predicted gene 14850	8 A2	2.5973	0.0148		
10361234	NM_008288	Hsd11b1	hydroxysteroid 11-beta dehydrogenase 1	1 H6	2.5957	0.0096		
10507171	NM_201640	Cyp4a31	cytochrome P450, family 4, subfamily a, polypeptide 31	4 D1	2.575	0.0484		
10570732	NM_001177528	Gm15315	predicted gene 15315	8 A2 8	2.5592	0.0098		
10599826	NM_007979	F9	coagulation factor IX	X A6-A7 X 22.0 cM	2.5474	0.0143		
10578916	NM_025436	Sc4mol	sterol-C4-methyl oxidase-like	8 B3.1	2.5379	0.0023		

Table A1. Continued.

Probe set ID	Gene accession	Gene symbol	Gene description	Cytoband	AJ CBDL vs sham FC	AJ CBDL vs sham FDR	B6 CBDL vs sham FC	B6 CBDL vs sham FDR
10399365	NM_177802	Slc7a15	solute carrier family 7 (cationic amino acid transporter, y+ system), member 15	12 A1.1	2.5357	0.0361		
10570693	NM_007851	Defa5	defensin, alpha, 5	8 A2	2.5181	0.0129		
10497590	NM_007963	Mecom	MDS1 and EVI1 complex locus	3 A3 3 14.4 cM	2.5047	0.0091		
10545881	NM_053096	Cml2	camello-like 2	6 C3	2.5013	0.027		
10478523	—	—	—	—	2.4962	0.0021		
10454944	NM_201256	Eif4ebp3	eukaryotic translation initiation factor 4E binding protein 3	18 B2	2.4951	0.0117		
10386683	NM_026183	Slc47a1	solute carrier family 47, member 1	11 B2	2.4534	0.0067		
10365559	NM_010512	Igf1	insulin-like growth factor 1	10 C1 10 48.0 cM	2.4375	0.0041		
10500555	NM_001161742	Hsd3b3	hydroxy-delta-5-steroid dehydrogenase, 3 beta- and steroid delta-isomerase 3	3 F2.2 3 49.1 cM	2.4177	0.0094		
10513412	NM_008648	Mup4	major urinary protein 4	4 B3 4 27.8 cM	2.3986	5.00E-04		
10491846	—	—	—	—	2.3936	0.0128		
10537306	NM_145364	Akr1d1	aldo-keto reductase family 1, member D1	6 B1	2.3924	0.0045		
10589099	NM_029634	Ip6k2	inositol hexaphosphate kinase 2	9 F2	2.3776	0.0021		
10594825	NM_022026	Aqp9	aquaporin 9	9 D	2.3723	0.0412		
10519578	NM_008830	Abcb4	ATP-binding cassette, sub-family B (MDR/TAP), member 4	5 A1 5 1.0 cM	2.3672	0.0297		
10590957	NM_010242	Fut4	fucosyltransferase 4	9 A2 9 3.0 cM	2.3611	0.0019		
10447317	NM_010137	Epas1	endothelial PAS domain protein 1	17 E4	2.2998	0.0142		
10352000	NM_133809	Kmo	kynurenine 3-monooxygenase (kynurenine 3-hydroxylase)	1 H4	2.2966	0.0301		
10360840	NM_001081361	Mosc1	MOCO sulphurase C-terminal domain containing 1	—	2.2607	0.0105		
10570660	NM_001177481	Gm10104	predicted gene 10104	8 A2 8	2.2377	0.0163		
10386460	NM_008819	Pemt	phosphatidylethanolamine N-methyltransferase	11 B1.3 11 31.0 cM	2.2274	0.0265		
10576901	NM_011388	Slc10a2	solute carrier family 10, member 2	8 A1.1 8 2.0 cM	2.2212	0.0253		
10530319	NM_001038999	Atp8a1	ATPase, aminophospholipid transporter (APLT), class I, type 8A, member 1	5 C3.1	2.1827	0.0152		
10502050	NM_027808	Alpk1	alpha-kinase 1	3 H1	2.1604	0.04		
10381096	NM_010517	Igfbp4	insulin-like growth factor binding protein 4	11 D	2.1452	0.0025		

Table A1. Continued.

Probe set ID	Gene accession	Gene symbol	Gene description	Cytoband	AJ CBDL vs sham FC	AJ CBDL vs sham FDR	B6 CBDL vs sham FC	B6 CBDL vs sham FDR
10408689	NM_153529	Nrn1	neuritin 1	13 A3.3	2.1125	0.0301		
10587266	NM_010295	Gclc	glutamate-cysteine ligase, catalytic subunit	9 D-E 9 42.0 cM	2.1067	0.0473		
10429588	NM_001039720	9030619P08Rik	RIKEN cDNA 9030619P08 gene	15 D3	2.1009	0.0025		
10537146	NM_008012	Akr1b8	aldo-keto reductase family 1, member B8	6 B1 6 13.0 cM	2.0926	0.0397		
10576774	NM_029465	Clec4g	C-type lectin domain family 4, member g	8 A1.1	2.0888	0.0367		
10542592	NR_033555	Gm10400	predicted gene 10400	—	2.0729	0.0104		
10496605	NM_173763	Ccbl2	cysteine conjugate-beta lyase 2	3 H1	2.0685	0.0222		
10358299	NM_001029977	EG214403	predicted gene, EG214403	1 F	2.0607	0.0386		
10494023	NM_011281	Rorc	RAR-related orphan receptor gamma	3 F2	2.0501	0.0013		
10357363	NM_001081756	Nckap5	NCK-associated protein 5	1 E3	2.0191	0.023		
10506452	AY512949	AY512949	cDNA sequence AY512949	—	2.0161	0.0416		
10512895	NM_007519	Baat	bile acid-Coenzyme A: amino acid N-acyltransferase	4 B1 4 22.7 cM	2.0089	0.0204		
10388430	NM_011340	Serpinf1	serine (or cysteine) peptidase inhibitor, clade F, member 1	11 B5	2.0036	0.0181		
10454198	NM_026301	Rnf125	ring finger protein 125	18 A2	2.003	0.0053		
10606989	NM_001077364	Tsc22d3	TSC22 domain family, member 3	X F1	1.9909	0.0197		
10418455	NM_008406	Itih1	inter-alpha trypsin inhibitor, heavy chain 1	14 A2-C1	1.9848	0.0374		
10365482	NM_011595	Timp3	tissue inhibitor of metalloproteinase 3	10 C1-D1 10 47.0 cM	1.9692	0.0355		
10388440	NM_008878	Serpinf2	serine (or cysteine) peptidase inhibitor, clade F, member 2	11 B5	1.9646	0.043		
10372682	NM_029875	Slc35e3	solute carrier family 35, member E3	10 D2	1.9641	0.0062		
10571657	NM_007981	Acs1	acyl-CoA synthetase long-chain family member 1	8 B2	1.9589	0.0041		
10581650	NM_011998	Chst4	carbohydrate (chondroitin 6/keratan) sulfotransferase 4	—	1.9469	0.039		
10394990	NM_026037	Mboat2	membrane bound O-acyltransferase domain containing 2	12 A1.3	1.9401	0.0244		
10596072	NM_001161362	Ppp2r3a	protein phosphatase 2, regulatory subunit B'', alpha	9 E4	1.9318	0.0021		
10411332	NM_008255	Hmgcr	3-hydroxy-3-methylglutaryl-Coenzyme A reductase	13 D1 13 49.0 cM	1.9292	0.0013		
10571840	NM_008278	Hpgd	hydroxyprostaglandin dehydrogenase 15 (NAD)	8 B3.2	1.9235	0.0025		

Table A1. Continued.

Probe set ID	Gene accession	Gene symbol	Gene description	Cytoband	AJ CBDL vs sham FC	AJ CBDL vs sham FDR	B6 CBDL vs sham FC	B6 CBDL vs sham FDR
10435787	—	—	—	—	1.9234	0.0109		
10555438	NM_199012	Fchsd2	FCH and double SH3 domains 2	7 E3	1.9147	0.0156		
10436100	NM_181596	Retnlg	resistin like gamma	16 B5 16 32.5 cM	1.9126	0.0028		
10542594	AY512955	Gm10210	predicted gene 10210	—	1.9107	0.047		
10554693	NM_023377	Stard5	StAR-related lipid transfer (START) domain containing 5	7 D3	1.903	0.0204		
10391744	AK135410	Gpatch8	G patch domain containing 8	11 E1	1.9025	0.0148		
10560624	NM_009696	Apoe	apolipoprotein E	7 A3 7 4.0 cM	1.8965	0.0301		
10542880	BC048711	4833442J19Rik	RIKEN cDNA 4833442J19 gene	6 G3	1.8917	0.0144		
10461150	—	—	—	—	1.8816	0.0397		
10585982	NM_173018	Myo9a	myosin IXa	9 B	1.8764	0.019		
10547469	NM_001037155	Hsn2	hereditary sensory neuropathy, type II	6 F1	1.8743	0.0152		
10482762	NM_145360	Idi1	isopentenyl-diphosphate delta isomerase	13 A1	1.8722	0.0143		
10411147	NM_022884	Bhmt2	betaine-homocysteine methyltransferase 2	13 C3 13 49.0 cM	1.8637	0.0317		
10364038	NM_133995	Upb1	ureidopropionase, beta	10 C1	1.8607	0.0099		
10382888	AK171830	2810008D09Rik	RIKEN cDNA 2810008D09 gene	—	1.8559	0.0272		
10485170	NM_009963	Cry2	cryptochrome 2 (photolyase-like)	2 E	1.8553	0.0324		
10594988	NM_015806	Mapk6	mitogen-activated protein kinase 6	9 D 9 38.0 cM	1.8546	0.0327		
10535938	NM_133898	N4bp2l1	NEDD4 binding protein 2-like 1	5 G3	1.8517	0.0189		
10556769	NM_016870	Acsn3	acyl-CoA synthetase medium -chain family member 3	7 F3	1.8511	0.0207		
10401149	NM_013738	Plek2	pleckstrin 2	12 D2	1.8429	0.0098		
10599192	NM_028894	Lonrf3	LON peptidase N-terminal domain and ring finger 3	X A2	1.8374	0.035		
10391746	NM_001159492	Gpatch8	G patch domain containing 8	11 E1	1.8331	0.0248		
10403413	NM_145360	Idi1	isopentenyl-diphosphate delta isomerase	13 A1	1.8228	0.0272		
10580955	—	—	—	—	1.8221	0.0277		
10396730	—	—	—	—	1.8218	0.0374		
10508800	AY140896	Gm3579	predicted gene 3579	4 D2.3 4	1.8214	0.0197		
10573865	AY140896	Gm3579	predicted gene 3579	4 D2.3 4	1.8214	0.0197		
10558961	NM_053082	Tspan4	tetraspanin 4	7 F5	1.8183	0.0132		
10350753	NM_008131	Glul	glutamate-ammonia ligase (glutamine synthetase)	—	1.817	0.0285		
10351043	NR_028543	Snord47	small nucleolar RNA, C/D box 47	1 1	1.8156	0.0327		
10377439	NM_001159367	Per1	period homolog 1 (Drosophila)	11 B	1.8092	0.0359		

Table A1. Continued.

Probe set ID	Gene accession	Gene symbol	Gene description	Cytoband	AJ CBDL vs sham FC	AJ CBDL vs sham FDR	B6 CBDL vs sham FC	B6 CBDL vs sham FDR
10520388	NM_028234	Rbm33	RNA binding motif protein 33	5 B1	1.8056	0.0379		
10370931	NM_021462	Mknk2	MAP kinase-interacting serine/threonine kinase 2	10 C1	1.7989	0.0023		
10582658	NM_007428	Agt	angiotensinogen (serpin peptidase inhibitor, clade A, member 8)	8 E2 8 68.0 cM	1.7834	0.0217		
10472860	NM_019688	Rapgef4	Rap guanine nucleotide exchange factor (GEF) 4	2 C3	1.7824	0.0118		
10505489	NM_021362	Pappa	pregnancy-associated plasma protein A	4 C1 4 32.2 cM	1.7809	0.0012		
10377751	NM_009714	Asgr1	asialoglycoprotein receptor 1	11 B3 11 37.0 cM	1.7793	0.0146		
10351224	NM_007976	F5	coagulation factor V	1 H2.2 1 86.6 cM	1.7735	0.0277		
10372988	NM_011391	Slc16a7	solute carrier family 16 (monocarboxylic acid transporters), member 7	10 D3	1.7729	0.0311		
10351259	NM_054087	Slc19a2	solute carrier family 19 (thiamine transporter), member 2	1 H2.2 1 87.0 cM	1.7698	0.0242		
10409876	NM_007796	Ctla2a	cytotoxic T lymphocyte -associated protein 2 alpha	13 B2 13 36.0 cM	1.7598	0.0424		
10410877	NM_001081176	Polr3g	polymerase (RNA) III (DNA directed) polypeptide G	13 C3	1.7388	0.0345		
10424686	BC025446	BC025446	cDNA sequence BC025446	15 D3	1.7378	0.0152		
10351533	NM_009803	Nr1i3	nuclear receptor subfamily 1, group I, member 3	1 H3 1 92.6 cM	1.7285	0.0341		
10533050	NM_030704	Hspb8	heat shock protein 8	5 F 5 59.0 cM	1.716	0.0394		
10496872	NM_133222	Eltf1	EGF, latrophilin seven transmembrane domain containing 1	3 H3-H4	1.7157	0.0233		
10518743	NM_173371	H6pd	hexose-6-phosphate dehydrogenase (glucose 1-dehydrogenase)	4 E2 4 78.4 cM	1.7094	0.0165		
10487021	NM_011774	Slc30a4	solute carrier family 30 (zinc transporter), member 4	2 E5 2 69.0 cM	1.7066	0.0161		
10595622	—	—	—	—	1.7056	0.0342		
10595636	—	—	—	—	1.7056	0.0342		
10595626	—	—	—	—	1.7034	0.029		
10446425	—	—	—	—	1.7003	0.0214		

Table A1. Continued.

Probe set ID	Gene accession	Gene symbol	Gene description	Cytoband	AJ CBDL vs sham FC	AJ CBDL vs sham FDR	B6 CBDL vs sham FC	B6 CBDL vs sham FDR
10473160	NM_080558	Ssfa2	sperm specific antigen 2	2 D	1.6908	0.0159		
10375229	—	—	—	—	1.6902	0.0112		
10592938	NM_138951	Ttc36	tetratricopeptide repeat domain 36	9 A5.2	1.6901	0.04		
10394699	NM_009072	Rock2	Rho-associated coiled-coil containing protein kinase 2	12 A3	1.6898	0.0376		
10354085	NM_019570	Rev1	REV1 homolog (S. cerevisiae)	1 B	1.6849	0.0097		
10462922	NM_019588	Plce1	phospholipase C, epsilon 1	19 D1	1.6829	0.032		
10395259	NM_021524	Nampt	nicotinamide phosphoribosyltransferase	12 B1	1.676	0.0284		
10597875	NM_010012	Cyp8b1	cytochrome P450, family 8, subfamily b, polypeptide 1	9 F4 9 71.0 cM	1.6755	0.013		
10344809	NM_026493	Cspp1	centrosome and spindle pole associated protein 1	1 A2	1.6735	0.0484		
10347748	NM_028817	Acsl3	acyl-CoA synthetase long-chain family member 3	1 C4 1 24.1 cM	1.6733	0.019		
10375216	NM_145962	Pank3	pantothenate kinase 3	11 A4	1.6733	0.013		
10545877	NM_023455	Nat8	N-acetyltransferase 8 (GCN5-related, putative)	6 C3	1.6673	0.0378		
10374453	NM_008131	Glul	glutamate-ammonia ligase (glutamine synthetase)	—	1.666	0.0345		
10515690	NM_198170	Szt2	seizure threshold 2	4 D2.1	1.6601	0.0207		
10591612	NM_177030	Dock6	dedicator of cytokinesis 6	9 A3	1.6594	0.0225		
10389214	NM_011338	Ccl9	chemokine (C-C motif) ligand 9	11 C 11 47.4 cM	1.6564	0.0355		
10587688	—	—	—	—	1.6554	0.0277		
10595620	—	—	—	—	1.6554	0.0277		
10366275	—	—	—	—	1.6481	0.0095		
10607089	NM_207625	Acsl4	acyl-CoA synthetase long-chain family member 4	X F2	1.647	0.0484		
10379820	NM_133360	Acaca	acetyl-Coenzyme A carboxylase alpha	11 C	1.6452	0.0014		
10414537	NM_001161731	Ang	angiogenin, ribonuclease, RNase A family, 5	14 B-C1 14 18.0 cM	1.6406	0.0094		
10505779	NM_139306	Acer2	alkaline ceramidase 2	4 C4	1.6403	0.0141		
10564183	AF241256	Snord116	small nucleolar RNA, C/D box 116 cluster	7 C 7 29.0 cM	1.6393	0.0126		

Table A1. Continued.

Probe set ID	Gene accession	Gene symbol	Gene description	Cytoband	AJ CBDL vs sham FC	AJ CBDL vs sham FDR	B6 CBDL vs sham FC	B6 CBDL vs sham FDR
10544573	NM_027852	Rarres2	retinoic acid receptor responder (tazarotene induced) 2	6 B2.3	1.6174	0.0361		
10472436	NM_020283	B3galt1	UDP-Gal:betaGlcNAc beta 1,3-galactosyltransferase, polypeptide 1	2 C3	1.6168	0.0376		
10515399	NM_013807	Plk3	polo-like kinase 3 (Drosophila)	4 D1	1.616	0.039		
10407876	NM_138654	5033411D12Rik	RIKEN cDNA 5033411D12 gene	13 A2	1.6108	0.0317		
10478847	NM_001081005	1500012F01Rik	RIKEN cDNA 1500012F01 gene	2 H3	1.6077	0.0445		
10362896	NM_009846	Cd24a	CD24a antigen	10 B2 10 26.0 cM	1.6059	0.0272		
10535956	NM_001163493	Stard13	StAR-related lipid transfer (START) domain containing 13	5 G3	1.6025	0.0225		
10371400	NM_007771	Cry1	cryptochrome 1 (photolyase-like)	10 C 10 46.0 cM	1.5989	0.0109		
10540122	NM_009320	Slc6a6	solute carrier family 6 (neurotransmitter transporter, taurine), member 6	6 D1 6 38.2 cM	1.5937	0.0136		
10580953	—	—	—	—	1.5913	0.0232		
10356082	NM_011636	Plscr1	phospholipid scramblase 1	9 E3.3	1.5899	0.036		
10453272	NM_001001806	Zfp36l2	zinc finger protein 36, C3H type-like 2	17 E4	1.5897	0.013		
10488322	NM_001033348	Ralgapa2	Ral GTPase activating protein, alpha subunit 2 (catalytic)	2 G1	1.5885	0.0019		
10462406	NM_001081319	C030046E11Rik	RIKEN cDNA C030046E11 gene	19 C1	1.5858	0.0471		
10382797	NM_176902	Fam100b	family with sequence similarity 100, member B	11 E2	1.583	0.023		
10346328	XR_031547	Gm8292	predicted gene 8292	1 C1.2	1.5828	0.0066		
10459766	NR_028560	Scarna17	small Cajal body-specific RNA 17	18 18	1.5813	0.0232		
10461642	NR_028560	Scarna17	small Cajal body-specific RNA 17	18 18	1.5813	0.0232		
10474545	NM_133649	Slc12a6	solute carrier family 12, member 6	2 E3	1.5812	0.0361		
10471503	BC110660	Taf1d	TATA box binding protein (Tbp)-associated factor, RNA polymerase I, D	9 A3	1.5797	0.0352		
10572865	NM_027837	Isx	intestine specific homeobox	8 C2	1.5776	0.0224		
10357345	NM_172484	Nckap5	NCK-associated protein 5	1 E3	1.5726	0.0374		
10501494	NM_001042711	Amy2a5	amylase 2a5	3 F3 3 50.0 cM	1.5715	0.015		
10558295	ENSMUST00000106157	Zranb1	zinc finger, RAN-binding domain containing 1	7 F3	1.5699	0.0362		

Table A1. Continued.

Probe set ID	Gene accession	Gene symbol	Gene description	Cytoband	AJ CBDL vs sham FC	AJ CBDL vs sham FDR	B6 CBDL vs sham FC	B6 CBDL vs sham FDR
10553829	NR_003376	Gm7367	1110014K08Rik pseudogene	7 C 7	1.5663	0.0376		
10553831	NR_003376	Gm7367	1110014K08Rik pseudogene	7 C 7	1.5663	0.0376		
10557233	NM_144925	Tnrc6a	trinucleotide repeat containing 6a	7 F3	1.5644	0.0447		
10439667	NM_145389	BC016579	cDNA sequence, BC016579	16 B5	1.5633	0.0355		
10354168	NM_018775	Tbc1d8	TBC1 domain family, member 8	1 B	1.5603	0.0205		
10418169	ENSMUST00000079800 // ENSMUST00000079800	1700054O19Rik // 1700054O19Rik	RIKEN cDNA 1700054O19 gene // RIKEN cDNA 1700054O19 gene	14 A3 // 14 A3	1.5539	0.0023		
10509063	NM_178257	Il22ra1	interleukin 22 receptor, alpha 1	4 D3 4 62.0 cM	1.5466	0.0232		
10391732	NM_001159492	Gpatch8	G patch domain containing 8	11 E1	1.5421	0.0168		
10399198	NM_019744	Ncoa4	nuclear receptor coactivator 4	14 B	1.5412	0.0444		
10512774	NM_178893	Coro2a	coronin, actin binding protein 2A	4 B1	1.5393	0.0307		
10485633	ENSMUST00000099651	Gm10796	predicted gene 10796	—	1.5366	0.0286		
10350758	AK080751	A930039A15Rik	RIKEN cDNA A930039A15 gene	—	1.5361	0.044		
10427461	NM_001136079	Ptger4	prostaglandin E receptor 4 (subtype EP4)	15 A1 15 6.4 cM	1.5341	0.0233		
10417887	NM_029104	Zmynd17	zinc finger, MYND domain containing 17	14 B	1.531	0.0494		
10436209	NM_001033238	Cblb	Casitas B-lineage lymphoma b	16 B5	1.5287	0.0345		
10587792	NM_011636	Plscr1	phospholipid scramblase 1	9 E3.3	1.5275	0.0242		
10469300	NM_177268	Ankrd16	ankyrin repeat domain 16	2 A1	1.5231	0.0313		
10497487	—	—	—	—	1.5217	0.0217		
10510286	NM_027985	Mad2l2	MAD2 mitotic arrest deficient-like 2 (yeast)	4 E1	1.52	0.0152		
10475866	NM_207680	Bcl2l11	BCL2-like 11 (apoptosis facilitator)	2 F3-G1	1.5187	0.0194		
10497421	NM_080634	Hps3	Hermansky-Pudlak syndrome 3 homolog (human)	3 A2 3 12.5 cM	1.5153	0.0272		
10538356	NM_001163640	Chn2	chimerin (chimaerin) 2	6 B3	1.5142	0.0215		
10475946	NM_178404	Zc3h6	zinc finger CCCCH type containing 6	2 F1	1.5139	0.0465		
10584350	NM_009429	Tpt1	tumor protein, translationally-controlled 1	14 D3	1.5134	0.0362		
10523856	—	—	—	—	1.5131	0.0416		
10564159	AF241256	Snord116	small nucleolar RNA, C/D box 116 cluster	7 C 7 29.0 cM	1.5126	0.0148		
10559916	—	—	—	—	1.5073	0.0309		
10410513	NM_001040692	Slc6a18	solute carrier family 6 (neurotransmitter transporter), member 18	13 C1 13 42.0 cM	1.506	0.0469		
10413839	NM_001033988	Ncoa4	nuclear receptor coactivator 4	14 B	1.5054	0.048		

Table A1. Continued.

Probe set ID	Gene accession	Gene symbol	Gene description	Cytoband	AJ CBDL vs sham FC	AJ CBDL vs sham FDR	B6 CBDL vs sham FC	B6 CBDL vs sham FDR
10459768	—	—	—	—	1.5005	0.0316		
10562234	NM_001110252	Hpn	hepsin	7 B1	1.4972	0.0454		
10407370	NM_001113550	4833420G17Rik	RIKEN cDNA 4833420G17 gene	13 D2.3	1.4954	0.0245		
10517703	—	—	—	—	1.4948	0.0146		
10497441	NM_013755	Gyg	glycogenin	3 A2 3 12.5 cM	1.4893	0.0056		
10470959	NM_172267	Phyhd1	phytanoyl-CoA dioxygenase domain containing 1	2 B	1.4891	0.0376		
10601755	NM_019865	Rpl36a	ribosomal protein L36A	X E3	1.4875	0.0384		
10355050	NM_001045513	Raph1	Ras association (RalGDS/AF-6) and pleckstrin homology domains 1	1 C2	1.4843	0.0308		
10514500	NM_001004141	Cyp2j11	cytochrome P450, family 2, subfamily j, polypeptide 11	4 C5	1.483	0.045		
10497399	NM_001122759	Pde7a	phosphodiesterase 7A	3 A2 3 7.0 cM	1.4697	0.0106		
10532040	NM_026856	Zfp644	zinc finger protein 644	5 E5 5 56.0 cM	1.4674	0.0484		
10421972	NM_019865	Rpl36a	ribosomal protein L36A	X E3	1.467	0.0489		
10399478	NM_015763	Lpin1	lipin 1	12 A1.1 12 9.0 cM	1.4665	0.0214		
10438358	NM_213614	5-Sep	septin 5	16 A3 16 11.42 cM	1.4654	0.0468		
10544219	NM_139294	Braf	Braf transforming gene	6 B1 6 15.5 cM	1.4639	0.0078		
10358894	NM_146126	Sord	sorbitol dehydrogenase	2 E5 2 66.0 cM	1.4618	0.0277		
10401997	NM_011877	Ptpn21	protein tyrosine phosphatase, non-receptor type 21	12 F1	1.4616	0.0405		
10475437	NM_146126	Sord	sorbitol dehydrogenase	2 E5 2 66.0 cM	1.4599	0.0325		
10379034	NM_026708	Tlcd1	TLC domain containing 1	11 B5	1.4516	0.0339		
10497935	—	—	—	—	1.4454	0.0361		
10389025	NM_177390	Myo1d	myosin ID	11 B5 11 46.0 cM	1.443	0.0454		
10389022	NM_177390	Myo1d	myosin ID	11 B5 11 46.0 cM	1.4428	0.0447		
10396956	NM_018814	Pcnx	pecanex homolog (Drosophila)	12 D1	1.4386	0.0122		
10462346	NM_021525	Rcl1	RNA terminal phosphate cyclase-like 1	19 C1	1.4359	0.0151		
10352416	NM_130890	Capn8	calpain 8	1 H4	1.4317	0.0233		
10592001	NM_011176	St14	suppression of tumorigenicity 14 (colon carcinoma)	9 A4 9 17.0 cM	1.4289	0.0123		
10507110	—	—	—	—	1.4264	0.0448		
10552030	NM_008085	Gapdhs	glyceraldehyde-3-phosphate dehydrogenase, spermatogenic	7 B1	1.4162	0.0437		
10447429	ENSMUST00000072072	Gm4832	predicted gene 4832	17 E4	1.4137	0.035		
10520371	NM_028234	Rbm33	RNA binding motif protein 33	5 B1	1.4117	0.045		

Table A1. Continued.

Probe set ID	Gene accession	Gene symbol	Gene description	Cytoband	AJ CBDL vs sham FC	AJ CBDL vs sham FDR	B6 CBDL vs sham FC	B6 CBDL vs sham FDR
10402117	NM_153587	Rps6ka5	ribosomal protein S6 kinase, polypeptide 5	12 E	1.4072	0.048		
10481827	NM_001085507	Zbtb34	zinc finger and BTB domain containing 34	2 B	1.4071	0.0194		
10526656	NM_146164	Lrch4	leucine-rich repeats and calponin homology (CH) domain containing 4	5 G2	1.404	0.0447		
10582811	NM_001164598	Irf2bp2	interferon regulatory factor 2 binding protein 2	8 E2	1.3943	0.0286		
10493343	—	—	—	—	1.3926	0.0441		
10474725	NM_013719	Eif2ak4	eukaryotic translation initiation factor 2 alpha kinase 4	—	1.3874	0.0301		
10489377	NM_012032	Serinc3	serine incorporator 3	2 H3	1.3784	0.0274		
10480570	NM_001162485	Arrdc1	arrestin domain containing 1	2 A3	1.3734	0.0478		
10366446	NM_146010	Tspan8	tetraspanin 8	10 D2	1.3733	0.0324		
10346970	NM_011086	Pikfyve	phosphoinositide kinase, FYVE finger containing	1 C2	1.3711	0.0175		
10384423	NM_172496	Cobl	cordon-bleu	11 A1 11 6.5 cM	1.3708	0.048		
10476443	NM_013829	Plcb4	phospholipase C, beta 4	2 F3 2 77.0 cM	1.3705	0.0333		
10534889	NM_178162	Agfg2	ArfGAP with FG repeats 2	5 G2	1.369	0.0181		
10518428	NM_011929	Clcn6	chloride channel 6	4 76.4 cM	1.3681	0.0262		
10542264	NM_001163445	2700089E24Rik	RIKEN cDNA 2700089E24 gene	6 G1	1.3677	0.045		
10497485	—	—	—	—	1.3662	0.0333		
10349065	NM_001122676	Zcchc2	zinc finger, CCHC domain containing 2	1 E2.1	1.3603	0.0286		
10477311	NM_001039939	Asxl1	additional sex combs like 1 (Drosophila)	2 H1	1.3592	0.0395		
10432122	NM_001170711	Asb8	ankyrin repeat and SOCS box-containing 8	15 F2	1.3504	0.0362		
10567229	NM_001031814	Smg1	SMG1 homolog, phosphatidylinositol 3-kinase-related kinase (C. elegans)	7 F2	1.3481	0.0485		
10376312	NM_028451	Larp1	La ribonucleoprotein domain family, member 1	11 B2	1.3375	0.0311		
10503161	NM_001081417	Chd7	chromodomain helicase DNA binding protein 7	4 A1 4 1.0 cM	1.3312	0.0407		
10587150	NM_001081322	Myo5c	myosin VC	9 D	1.3133	0.0489		

Table A1. Continued.

Probe set ID	Gene accession	Gene symbol	Gene description	Cytoband	AJ CBDL vs sham FC	AJ CBDL vs sham FDR	B6 CBDL vs sham FC	B6 CBDL vs sham FDR
10476033	NM_183262	Stk35	serine/threonine kinase 35	2 F1	1.2947	0.0412		
10466530	NM_001163144	Pcsk5	proprotein convertase subtilisin/kexin type 5	19 B 19 18.0 cM	1.2894	0.0362		
10478219	NM_021280	Plcg1	phospholipase C, gamma 1	2 H2 2 92.0 cM	1.2708	0.0381		
10367919	NM_029075	Stx11	syntaxin 11	10 A1	−1.2794	0.048		
10605319	NM_145405	Ubl4	ubiquitin-like 4	X A7.3 X 29.9 cM	−1.2895	0.048		
10508089	NM_025544	Mrps15	mitochondrial ribosomal protein S15	4 D2.1	−1.2959	0.0479		
10591482	NM_016679	Keap1	kelch-like ECH -associated protein 1	9 A3	−1.298	0.0397		
10591739	NM_001102404	Acp5	acid phosphatase 5, tartrate resistant	9 A3 9 6.0 cM	−1.3007	0.0272		
10551159	XR_034166	Gm4607	predicted gene 4607	7 A3 7	−1.3016	0.0479		
10413222	NM_134084	Ppif	peptidylprolyl isomerase F (cyclophilin F)	14 A3	−1.3037	0.048		
10356657	NM_024197	Ndufa10	NADH dehydrogenase (ubiquinone) 1 alpha subcomplex 10	1 D	−1.3055	0.0479		
10347672	NM_027886	Stk11ip	serine/threonine kinase 11 interacting protein	1 C3	−1.3059	0.0438		
10439695	NM_019754	Tagln3	transgelin 3	16 B5	−1.3087	0.0387		
10593591	NM_144784	Acat1	acetyl-Coenzyme A acetyltransferase 1	9 30.0 cM	−1.3115	0.0418		
10432866	NM_001003667	Krt77	keratin 77	15 F3	−1.3141	0.0484		
10378443	NM_001011851	Olfr412	olfactory receptor 412	11 B5	−1.3165	0.048		
10487629	NM_130884	Idh3b	isocitrate dehydrogenase 3 (NAD+) beta	2 F3	−1.3214	0.0265		
10432636	NM_174992	Smagp	small cell adhesion glycoprotein	15 F1	−1.3221	0.0376		
10543684	NR_030713	Mir183	microRNA 183	—	−1.3247	0.0355		
10411156	NM_029153	Scamp1	secretory carrier membrane protein 1	13 D1	−1.3284	0.036		
10585417	NM_029573	Idh3a	isocitrate dehydrogenase 3 (NAD+) alpha	9 A5.3	−1.3357	0.0367		
10415742	NM_027436	Mipep	mitochondrial intermediate peptidase	14 D1	−1.3368	0.0307		
10406205	NM_030711	Erap1	endoplasmic reticulum aminopeptidase 1	13 C1	−1.3442	0.0454		

Table A1. Continued.

Probe set ID	Gene accession	Gene symbol	Gene description	Cytoband	AJ CBDL vs sham FC	AJ CBDL vs sham FDR	B6 CBDL vs sham FC	B6 CBDL vs sham FDR
10449940	NM_022434	Cyp4f14	cytochrome P450, family 4, subfamily f, polypeptide 14	17 B1	−1.3479	0.0363		
10420225	NM_010780	Cma1	chymase 1, mast cell	14 C3 14 20.0 cM	−1.3516	0.0307		
10390685	NM_025661	Ormdl3	ORM1-like 3 (<i>S. cerevisiae</i>)	11 D	−1.3522	0.0445		
10484431	NM_025868	Tmx2	thioredoxin-related transmembrane protein 2	2 D	−1.3536	0.0486		
10515930	BC076608	AA415398	expressed sequence AA415398	4 D2.1	−1.3575	0.0362		
10607643	—	—	—	—	−1.3579	0.0374		
10386416	NM_001011789	Olfr222	olfactory receptor 222	11 B1.3	−1.3596	0.0447		
10488291	NM_015754	Rbbp9	retinoblastoma binding protein 9	2 G1-H1	−1.3617	0.032		
10447551	NM_027457	5730437N04Rik	RIKEN cDNA 5730437N04 gene	17 A1	−1.3687	0.0396		
10464128	NM_007611	Casp7	caspase 7	19 D2 19 50.0 cM	−1.3699	0.0383		
10377286	NM_001081566	Pik3r6	phosphoinositide-3-kinase, regulatory subunit 6	11 B3	−1.3731	0.0233		
10539472	NM_019542	Nagk	N-acetylglucosamine kinase	6 D1	−1.3736	0.0143		
10434191	NM_013711	Txnrd2	thioredoxin reductase 2	16 A3 16 11.2 cM	−1.3797	0.0324		
10369525	BC024943	2010107G23Rik	RIKEN cDNA 2010107G23 gene	10 B4	−1.3815	0.0461		
10465826	NM_001160356	Al462493	expressed sequence Al462493	19 A	−1.3869	0.0399		
10435617	NM_001042499	Rabl3	RAB, member of RAS oncogene family-like 3	16 B3	−1.3924	0.0387		
10495285	NM_019972	Sort1	sortilin 1	3 F3	−1.3932	0.035		
10447354	NM_025868	Tmx2	thioredoxin-related transmembrane protein 2	2 D	−1.3953	0.0338		
10575894	NM_026648	Lrrc50	leucine rich repeat containing 50	8 E1	−1.3988	0.0418		
10368893	NM_145743	Lace1	lactation elevated 1	10 B2 10 25.5 cM	−1.399	0.0265		
10470050	NM_007379	Abca2	ATP-binding cassette, sub-family A (ABC1), member 2	2 A2-B 2 12.6 cM	−1.4023	0.0316		
10566618	NM_206897	Olfr6	olfactory receptor 6	7 E3	−1.4057	0.0416		
10526514	NM_021719	Cldn15	claudin 15	5 G2	−1.4077	0.0418		
10483679	NM_001080707	Gpr155	G protein-coupled receptor 155	2 C3	−1.4079	0.035		
10476301	NM_001177833	Smox	spermine oxidase	2 F1	−1.408	0.0478		
10365116	NM_133964	Dohh	deoxyhypusine hydroxylase/monooxygenase	10 C1	−1.4203	0.0304		
10386086	NM_153079	Nmur2	neuromedin U receptor 2	11 B1.3	−1.4289	0.043		

Table A1. Continued.

Probe set ID	Gene accession	Gene symbol	Gene description	Cytoband	AJ CBDL vs sham FC	AJ CBDL vs sham FDR	B6 CBDL vs sham FC	B6 CBDL vs sham FDR
10442370	NM_019910	Dcpp1	demilune cell and parotid protein 1	17 A3.3 17 10.0 cM	−1.4357	0.043		
10593169	NM_023114	Apoc3	apolipoprotein C-III	9 A5.2 9 27.0 cM	−1.4359	0.0317		
10579508	NM_001164679	Ano8	anoctamin 8	8 B3.3	−1.4375	0.015		
10431300	NM_001142357	Alg12	asparagine-linked glycosylation 12 homolog (yeast, alpha-1, 6-mannosyltransferase)	15 E3	−1.4389	0.0334		
10585874	NM_010421	Hexa	hexosaminidase A	9 B 9 29.0 cM	−1.4394	0.0245		
10571302	NM_026432	Tmem66	transmembrane protein 66	8 A4	−1.4412	0.0307		
10519652	NR_003596	Gm6455	predicted gene 6455	5 A1	−1.4455	0.0286		
10397975	NM_026790	Ifi2711	interferon, alpha-inducible protein 27 like 1	12 E 12 51.0 cM	−1.4507	0.0331		
10362904	NM_130892	Rtn4ip1	reticulon 4 interacting protein 1	10 B2 10 29.0 cM	−1.4553	0.047		
10352767	NM_010892	Nek2	NIMA (never in mitosis gene a)-related expressed kinase 2	1 H6 1 103.0 cM	−1.4555	0.0145		
10480699	NM_031843	Dpp7	dipeptidylpeptidase 7	2 A3	−1.4566	0.0363		
10529454	ENSMUST00000069741	E130018O15Rik	RIKEN cDNA E130018O15 gene	5 B3	−1.4683	0.0429		
10600531	—	—	—	—	−1.4695	0.0218		
10426812	NM_010271	Gpd1	glycerol-3-phosphate dehydrogenase 1 (soluble)	15 56.8 cM	−1.4746	0.0375		
10519688	NR_003596	Gm6455	predicted gene 6455	5 A1	−1.4804	0.0063		
10518679	NM_133435	Nmnat1	nicotinamide nucleotide adenyltransferase 1	4 E2	−1.4814	0.048		
10357418	NM_001081078	Lct	lactase	1 E4	−1.4902	0.0333		
10559590	NM_207270	Ptprh	protein tyrosine phosphatase, receptor type, H	7 A1	−1.494	0.0286		
10525365	NM_001042489	Hvcn1	hydrogen voltage-gated channel 1	5 F	−1.4944	0.0376		
10424929	NM_172960	Adck5	aarF domain containing kinase 5	15 D3	−1.4964	0.043		
10351473	NM_001033499	Sh2d1b2	SH2 domain protein 1B2	1 H3	−1.4988	0.0061		
10547976	NM_145391	Tapbpl	TAP binding protein-like	6 F3	−1.5013	0.041		
10521391	NM_030721	Acox3	acyl-Coenzyme A oxidase 3, pristanoyl	—	−1.5034	0.0098		

Table A1. Continued.

Probe set ID	Gene accession	Gene symbol	Gene description	Cytoband	AJ CBDL vs sham FC	AJ CBDL vs sham FDR	B6 CBDL vs sham FC	B6 CBDL vs sham FDR
10490104	NM_011497	Aurka	aurora kinase A	2 H3 2 100.0 cM	−1.5077	0.035		
10411633	NM_008670	Naip1	NLR family, apoptosis inhibitory protein 1	13 D1-D3 13 54.0 cM	−1.5078	0.0232		
10450145	NM_013585	Psemb9	proteasome (prosome, macropain) subunit, beta type 9 (large multifunctional peptidase 2)	17 B1 17 18.59 cM	−1.5167	0.045		
10524681	NM_026933	Triap1	TP53 regulated inhibitor of apoptosis 1	5 F	−1.517	0.0058		
10490491	NM_008093	Gata5	GATA binding protein 5	2 H4 2 106.0 cM	−1.5174	0.0361		
10437655	NM_011955	Nubp1	nucleotide binding protein 1	16 A1 16 3.4 cM	−1.5217	0.0461		
10441530	NM_031395	Sytl3	synaptotagmin-like 3	17 A1	−1.5249	0.0443		
10562130	NM_194057	Ffar1	free fatty acid receptor 1	7 B1	−1.526	0.0014		
10463704	NM_020577	As3mt	arsenic (+3 oxidation state) methyltransferase	19 D1	−1.5357	0.0162		
10524878	NM_001033311	Vsig10	V-set and immunoglobulin domain containing 10	5 F	−1.5404	0.0046		
10393573	NM_011150	Lgals3bp	lectin, galactoside-binding, soluble, 3 binding protein	11 E	−1.5406	0.0119		
10606714	NM_013463	Gla	galactosidase, alpha	X E-F1 X 53.0 cM	−1.5428	0.0277		
10458547	NR_028061	Gm8615	glucosamine-6-phosphate deaminase 1 pseudogene	5 G3	−1.5451	0.0246		
10384378	NM_016672	Ddc	dopa decarboxylase	11 A1-A4 11 7.0 cM	−1.5472	0.043		
10429638	XR_032493	Gm9568	glyceraldehyde-3-phosphate dehydrogenase pseudogene	15 D3 15	−1.5502	0.0482		
10510516	NM_019741	Slc2a5	solute carrier family 2 (facilitated glucose transporter), member 5	4 E2	−1.5555	0.0065		
10565634	NM_008663	Myo7a	myosin VIIA	7 E2 7 48.1 cM	−1.5718	0.0053		
10524422	NM_010018	Dao	D-amino acid oxidase	5 F 5 65.0 cM	−1.575	0.0418		
10566583	AK172683	Gm8995	predicted gene 8995	7 E3	−1.5789	0.0371		
10391207	NM_030150	Dhx58	DEXH (Asp-Glu-X-His) box polypeptide 58	11 D 11 61.5 cM	−1.5797	0.0135		
10408879	NM_001033399	Gfod1	glucose-fructose oxidoreductase domain containing 1	13 A4	−1.5847	0.013		
10505954	NM_013690	Tek	endothelial-specific receptor tyrosine kinase	4 C5 4 43.6 cM	−1.5877	0.0422		

Table A1. Continued.

Probe set ID	Gene accession	Gene symbol	Gene description	Cytoband	AJ CBDL vs sham FC	AJ CBDL vs sham FDR	B6 CBDL vs sham FC	B6 CBDL vs sham FDR
10538082	NM_133764	Atp6v0e2	ATPase, H ⁺ transporting, lysosomal V0 subunit E2	6 B3	−1.5918	0.0041		
10545958	NM_013471	Anxa4	annexin A4	6 D1 6 38.0 cM	−1.596	0.0411		
10560474	NM_177691	Ppm1n	protein phosphatase, Mg2+/Mn2+ dependent, 1N (putative)	7 A3	−1.6066	0.0158		
10577792	NM_031257	Plekha2	pleckstrin homology domain -containing, family A (phosphoinositide binding specific) member 2	8 A2	−1.623	0.0343		
10455784	NM_026240	Gramd3	GRAM domain containing 3	18 D2	−1.6238	0.0361		
10467907	NM_145502	Erlin1	ER lipid raft associated 1	19 C3	−1.6274	0.0115		
10492102	NM_144895	Spg20	spastic paraplegia 20, spartin (Troyer syndrome) homolog (human)	3 C	−1.6317	0.0301		
10377927	NM_027445	Rnf167	ring finger protein 167	11 B4	−1.633	0.0209		
10404439	NM_011452	Serpib9b	serine (or cysteine) peptidase inhibitor, clade B, member 9b	13 A3.3 13 12.5 cM	−1.6346	0.0217		
10566585	ENSMUST00000098144	Gm1966	predicted gene 1966	7 E3	−1.6387	0.0248		
10587873	—	—	—	—	−1.6446	0.037		
10439068	NM_145932	Osta	organic solute transporter alpha	16 B3	−1.6448	0.035		
10376726	NM_001172112	Dhrs7b	dehydrogenase/reductase (SDR family) member 7B	11 B2	−1.6476	0.0062		
10469951	NM_176834	Rnf208	ring finger protein 208	2 A3	−1.6491	0.0225		
10548817	NM_025806	Plbd1	phospholipase B domain containing 1	6 G1	−1.654	0.0163		
10473356	NM_019949	Ube2l6	ubiquitin-conjugating enzyme E2L 6	2 E1	−1.6544	0.0048		
10501235	NM_026764	Gstm4	glutathione S-transferase, mu 4	3 F2.3	−1.6622	0.0309		
10474825	NM_026412	D2Ert750e	DNA segment, Chr 2, ERATO Doi 750, expressed	2 E5	−1.6757	0.0095		
10463716	NM_033569	Cnnm2	cyclin M2	19 C3 19 47.0 cM	−1.6797	0.0023		
10604337	—	—	—	—	−1.6798	0.0307		
10595081	NM_012033	Tinag	tubulointerstitial nephritis antigen	9 D	−1.6828	0.0065		

Table A1. Continued.

Probe set ID	Gene accession	Gene symbol	Gene description	Cytoband	AJ CBDL vs sham FC	AJ CBDL vs sham FDR	B6 CBDL vs sham FC	B6 CBDL vs sham FDR
10524621	NM_011854	Oasl2	2'-5' oligoadenylate synthetase-like 2	5 F	-1.687	0.0489		
10444810	ENSMUST00000105041	H2-Q1	histocompatibility 2, Q region locus 1	17 B1 17 19.14 cM	-1.6883	0.0032		
10584334	NM_011734	Siae	sialic acid acetyltransferase	9 A4 9 19.0 cM	-1.699	0.0032		
10582985	NM_009807	Casp1	caspase 1	9 A1 9 1.0 cM	-1.6991	0.0091		
10488185	NM_009751	Bfsp1	beaded filament structural protein 1, in lens-CP94	2 G	-1.7014	0.0096		
10491091	NM_009425	Tnfsf10	tumor necrosis factor (ligand) superfamily, member 10	3 A3	-1.7131	0.0053		
10583920	NM_026189	Eepd1	endonuclease/exonuclease/phosphatase family domain containing 1	9 A4	-1.7418	0.0179		
10378572	NM_027249	Tlcd2	TLC domain containing 2	11 B5	-1.7499	0.0309		
10383192	—	—	—	—	-1.7677	0.0205		
10559606	NM_023440	Tmem86b	transmembrane protein 86B	7 A1	-1.776	0.008		
10550740	NM_027839	Ceacam20	carcinoembryonic antigen-related cell adhesion molecule 20	7 A3	-1.7837	0.0219		
10486172	NM_001033136	Fam82a2	family with sequence similarity 82, member A2	2 E5	-1.7911	0.0045		
10482802	NM_139200	Cytip	cytohesin 1 interacting protein	2 C1.1	-1.798	0.0078		
10402347	NM_029803	Ifi2712a	interferon, alpha-inducible protein 27 like 2A	12 E	-1.807	0.0173		
10519196	NM_147776	Vwa1	von Willebrand factor A domain containing 1	—	-1.8075	0.0079		
10488636	NM_001039120	Defb26	defensin beta 26	2 H1	-1.8103	0.041		
10542857	NM_178797	Far2	fatty acyl CoA reductase 2	6 G3	-1.8273	0.0308		
10376832	NM_007413	Adora2b	adenosine A2b receptor	11 B2	-1.8282	0.0194		
10558265	NM_029609	Lhpp	phospholysine phosphohistidine inorganic pyrophosphate phosphatase	7 F4	-1.8296	0.001		
10569203	NM_001142681	Chid1	chitinase domain containing 1	7 F5	-1.8468	0.0112		
10571984	NM_001081215	Ddx60	DEAD (Asp-Glu-Ala-Asp) box polypeptide 60	8 B3.1	-1.8805	0.05		
10424221	NM_001081396	Wdr67	WD repeat domain 67	15 D1	-1.8879	0.0054		
10364134	NM_133184	Slc5a4a	solute carrier family 5, member 4a	10 C1	-1.9264	0.0251		

Table A1. Continued.

Probe set ID	Gene accession	Gene symbol	Gene description	Cytoband	AJ CBDL vs sham FC	AJ CBDL vs sham FDR	B6 CBDL vs sham FC	B6 CBDL vs sham FDR
10447904	NM_199252	Unc93a	unc-93 homolog A (<i>C. elegans</i>)	17 A1 17 7.8 cM	−1.9295	0.025		
10539186	NM_011259	Reg3a	regenerating islet -derived 3 alpha	6 C3 6 33.5 cM	−1.9355	0.0286		
10451287	NM_015783	Isg15	ISG15 ubiquitin -like modifier	4 E2 4	−1.936	0.013		
10447634	NM_001142539	Gm9992	predicted gene 9992	17 A1	−1.9524	0.0175		
10389261	NM_001037932	Gm11437	predicted gene 11437	11 C	−1.9832	0.0076		
10538590	NM_025992	Herc5	hect domain and RLD 5	6 C1 6	−1.9883	0.0089		
10510532	NM_001085529	Slc2a7	solute carrier family 2 (facilitated glucose transporter), member 7	4 E2 4	−2.0053	0.0136		
10385500	NM_008326	Irgm1	immunity-related GTPase family M member 1	11 B1.2	−2.0184	0.0234		
10587871	NM_198414	Paqr9	progesterin and adipoQ receptor family member IX	9 E3.3	−2.0207	0.0376		
10568568	NM_016978	Oat	ornithine aminotransferase	7 F3 7 63.0 cM	−2.0471	3.00E−04		
10467470	NM_019698	Aldh18a1	aldehyde dehydrogenase 18 family, member A1	19 C3	−2.3775	0.0079		
10425287	NM_134090	Kdelr3	KDEL (Lys-Asp-Glu-Leu) endoplasmic reticulum protein retention receptor 3	15 E1	−2.4335	0.0115		
10376324	NM_001135115	Gm12250	predicted gene 12250	11 B1.3	−2.4477	0.0311		
10443869	NM_024442	Cyp4f16	cytochrome P450, family 4, subfamily f, polypeptide 16	17 B1	−2.5218	0.0265		
10566571	NR_030719	Gm8979	very large inducible GTPase 1 pseudogene	7 E3	−2.6198	0.0145		
10390748	NM_172564	Tns4	tensin 4	11 D	−2.6277	0.0044		
10462618	NM_010501	Ifit3	interferon-induced protein with tetratricopeptide repeats 3	19 C3	−2.6278	0.0357		
10545200	ENSMUST00000101325	LOC100046894	similar to Igk-C protein	—	−2.6477	0.0473		
10499899	NM_009264	Sprr1a	small proline-rich protein 1A	3 F1 3 45.2 cM	−2.7972	0.0286		
10483074	NM_008100	Gcg	glucagon	2 C1.3 2 36.0 cM	−2.7977	0.0019		
10557300	NM_007474	Aqp8	aquaporin 8	7 F3 7 61.0 cM	−2.7985	8.00E−04		
10566578	NR_030719	Gm8979	very large inducible GTPase 1 pseudogene	7 E3	−2.8066	0.0095		
10430006	NM_028064	Slc39a4	solute carrier family 39 (zinc transporter), member 4	15 D3	−2.8188	0.0145		

Table A1. Continued.

Probe set ID	Gene accession	Gene symbol	Gene description	Cytoband	AJ CBDL vs sham FC	AJ CBDL vs sham FDR	B6 CBDL vs sham FC	B6 CBDL vs sham FDR
10390691	NM_145434	Nr1d1	nuclear receptor subfamily 1, group D, member 1	11 D	−3.298	3.00E−04		
10480633	NM_080854	Slc34a3	solute carrier family 34 (sodium phosphate), member 3	2 A3	−3.3614	0.013		
10566366	NM_199146	AI451617	expressed sequence AI451617	7 E3	−3.9279	0.0019		
10505451	NM_011016	Orm2	orosomucoid 2	4 C1 4 31.4 cM			3.9755	0.0307
10416057	NM_013492	Clu	clusterin	14 D1 14 28.0 cM			3.6483	0.0393
10452854	NM_053188	Srd5a2	steroid 5 alpha-reductase 2	17 E2			3.4167	7.00E−04
10367045	NM_009040	Rdh16	retinol dehydrogenase 16	10 D3			2.3984	0.0273
10523717	NM_009263	Spp1	secreted phosphoprotein 1	5 E5 5 56.0 cM			2.2985	0.0406
10464594	BC034269	BC021614	cDNA sequence BC021614	19 A			2.2581	0.011
10429140	NM_008681	Ndrg1	N-myc downstream regulated gene 1	15 D2			2.087	0.0273
10469609	NR_033225	Gm13375	predicted gene 13375	2 A3			2.0048	0.0294
10507671	NM_008190	Guca2a	guanylate cyclase activator 2a (guanylin)	4 D2.1 4 57.0 cM			1.8922	0.0482
10556113	NM_016809	Rbm3	RNA binding motif protein 3	X A1.1 X 2.0 cM			1.8115	0.0271
10359917	NM_010476	Hsd17b7	hydroxysteroid (17-beta) dehydrogenase 7	1 H3			1.7626	0.0467
10358454	NM_001166409	Rbm3	RNA binding motif protein 3	X A1.1 X 2.0 cM			1.7444	0.0294
10540034	NM_027406	Aldh1l1	aldehyde dehydrogenase 1 family, member L1	6 D1			1.7157	0.015
10371784	NM_001163700	Nr1h4	nuclear receptor subfamily 1, group H, member 4	10 C2 10 50.0 cM			1.7001	0.0435
10603469	NM_001166409	Rbm3	RNA binding motif protein 3	X A1.1 X 2.0 cM			1.6579	0.0273
10582310	NM_138656	Mvd	mevalonate (diphospho) decarboxylase	8 E1			1.6179	0.0287
10518568	—	—	—	—			1.5432	0.0336
10443898	NM_134127	Cyp4f15	cytochrome P450, family 4, subfamily f, polypeptide 15	17 B1			1.5311	0.0468
10344713	NM_016661	Ahcy	S-adenosylhomocysteine hydrolase	2 H1 2 89.0 cM			1.5215	0.0425
10488816	NM_016661	Ahcy	S-adenosylhomocysteine hydrolase	2 H1 2 89.0 cM			1.5127	0.0377
10439762	NM_016661	Ahcy	S-adenosylhomocysteine hydrolase	2 H1 2 89.0 cM			1.5089	0.0468
10605055	NM_028633	Haus7	HAUS augmin-like complex, subunit 7	X A7.3			1.5083	0.015

Table A1. Continued.

Probe set ID	Gene accession	Gene symbol	Gene description	Cytoband	AJ CBDL vs sham FC	AJ CBDL vs sham FDR	B6 CBDL vs sham FC	B6 CBDL vs sham FDR
10556169	NM_025344	Eif3f	eukaryotic translation initiation factor 3, subunit F	7 E3			1.418	0.0317
10413542	NM_009388	Tkt	transketolase	14 B1			1.4043	0.0425
10408850	NM_001111324	Neddd9	neural precursor cell expressed, developmentally down-regulated gene 9	13 A3.3-A4			-1.3853	0.0463
10489107	NM_018851	Samhd1	SAM domain and HD domain, 1	2 H2			-1.4139	0.0456
10516620	NM_010693	Lck	lymphocyte protein tyrosine kinase	4 D2.2 4 59.0 cM			-1.4259	0.0348
10513256	NM_010336	Lpar1	lysophosphatidic acid receptor 1	4 B3 4 16.0 cM			-1.434	0.0294
10604057	NR_033443	6-Sep	septin 6	X A2			-1.4532	0.0468
10588464	NR_029526	Mirlet7g	microRNA let7g	—			-1.464	0.0301
10432362	NM_026967	Rhebl1	Ras homolog enriched in brain like 1	15 F2			-1.49	0.017
10350173	NM_001130174	Tnnt2	troponin T2, cardiac	1 E4 1 60.0 cM			-1.4944	0.0425
10547906	NM_008479	Lag3	lymphocyte -activation gene 3	6 F2			-1.5108	0.0346
10420659	NM_025697	6330409N04Rik	RIKEN cDNA 6330409N04 gene	14 D1			-1.5451	0.0354
10352097	NM_027077	1700016C15Rik	RIKEN cDNA 1700016C15 gene	1 H3			-1.5503	0.0468
10409579	NM_019568	Cxcl14	chemokine (C-X-C motif) ligand 14	13 B1			-1.5799	0.0377
10355960	NM_009129	Scg2	secretogranin II	1 C4 1 43.6 cM			-1.6019	0.0178
10478633	NM_013599	Mmp9	matrix metalloproteinase 9	2 H1-H2 2 96.0 cM			-1.6069	0.0228
10501629	NM_001080818	Cdc14a	CDC14 cell division cycle 14 homolog A (S. cerevisiae)	3 G1			-1.6217	0.0425
10447056	NM_027455	Qpct	glutaminyl-peptide cyclotransferase (glutaminyl cyclase)	17 E3			-1.6326	0.0228
10407940	—	—	—	—			-1.6681	0.0294
10605355	—	—	—	—			-1.6826	0.0494
10593015	NM_009850	Cd3g	CD3 antigen, gamma polypeptide	9 A5.2 9 26.0 cM			-1.6893	0.0161
10464999	NM_028623	Cst6	cystatin E/M	19 A 19 4.0 cM			-1.7219	0.0456
10584821	NM_013487	Cd3d	CD3 antigen, delta polypeptide	9 A5.2 9 26.0 cM			-1.7359	0.0435

Table A1. Continued.

Probe set ID	Gene accession	Gene symbol	Gene description	Cytoband	AJ CBDL vs sham FC	AJ CBDL vs sham FDR	B6 CBDL vs sham FC	B6 CBDL vs sham FDR
10561927	NM_007467	Ap1p	amyloid beta (A4) precursor-like protein 1	7 B1 7 8.0 cM			−1.7367	0.0109
10552406	NM_024253	Nkg7	natural killer cell group 7 sequence	7 B2			−1.7501	0.0178
10366881	NM_007837	Ddit3	DNA-damage inducible transcript 3	10 D3			−1.7621	0.0344
10490923	NM_009801	Car2	carbonic anhydrase 2	3 A1 3 10.5 cM			−1.7726	0.0189
10428534	NM_032000	Trps1	trichorhinophalangeal syndrome I (human)	15 C 15 30.1 cM			−1.793	0.0494
10403821	ENSMUST00000103558	Tcrg-V3	T-cell receptor gamma, variable 3	—			−1.8213	0.0468
10516093	NM_007558	Bmp8a	bone morphogenetic protein 8a	4 D2.2 4 57.4 cM			−1.8392	0.0307
10513739	NM_011607	Tnc	tenascin C	4 C1 4 32.2 cM			−1.853	0.0348
10574166	NM_153507	Cpne2	copine II	8 C5			−1.857	0.0346
10542632	NM_010491	Iapp	islet amyloid polypeptide	6 G2 6 62.0 cM			−1.8827	0.0301
10541605	NM_020001	Clec4n	C-type lectin domain family 4, member n	6 F3 6 55.0 cM			−1.889	0.017
10402325	NM_023049	Asb2	ankyrin repeat and SOCS box-containing 2	12 E 12 50.0 cM			−1.9087	0.0492
10466200	NM_027836	Ms4a7	membrane-spanning 4-domains, subfamily A, member 7	19 A			−1.9359	0.0172
10404913	NM_026056	Cap2	CAP, adenylate cyclase -associated protein, 2 (yeast)	13 A5			−1.9619	0.0346
10420308	NM_013542	Gzmb	granzyme B	14 D3 14 20.5 cM			−1.9705	0.0294
10412211	NM_010370	Gzma	granzyme A	13 D 13 64.0 cM			−2.0182	0.0229
10463016	NM_028191	Cyp2c65	cytochrome P450, family 2, subfamily c, polypeptide 65	19 C3			−2.1252	0.0456
10551197	NM_009999	Cyp2b10	cytochrome P450, family 2, subfamily b, polypeptide 10	7 A3 7 6.5 cM			−2.5753	0.0138
10512999	NR_033139	AI427809	expressed sequence AI427809	4 B2			−2.5806	0.0109
10405063	NM_008760	Ogn	osteoglycin	13 A5			−2.6878	0.0346
10512949	NM_013454	Abca1	ATP-binding cassette, sub-family A (ABC1), member 1	4 A5-B3 4 23.1 cM			−2.753	0.0273
10366043	NM_026268	Dusp6	dual specificity phosphatase 6	10 C3			−3.0369	0.0224
10534493	NM_019577	Ccl24	chemokine (C-C motif) ligand 24	5 G1			−4.9474	0.0072
10463023	NM_001011707	Cyp2c66	cytochrome P450, family 2, subfamily c, polypeptide 66	19 C3			−5.082	0.015